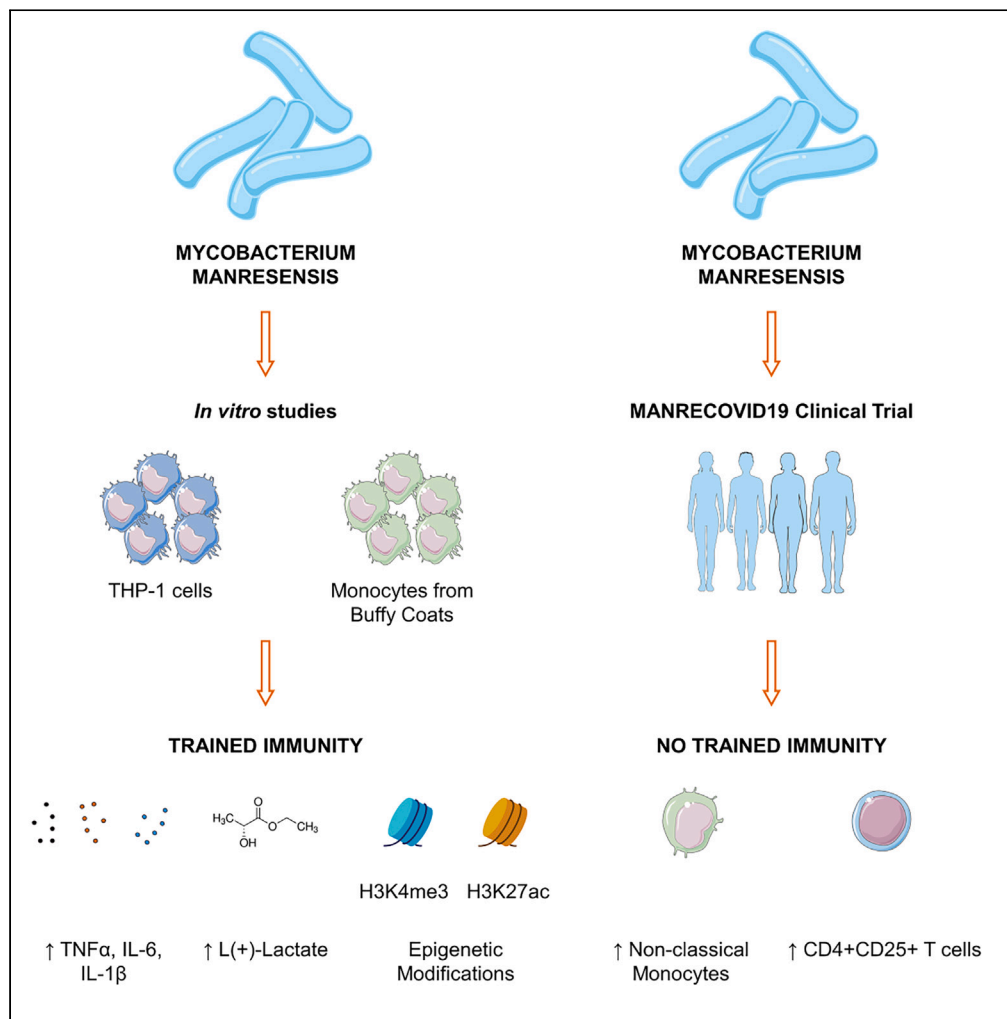


Article

Mycobacterium manresensis induces trained immunity in vitro



Miquel de Homdedeu, Lidia Sanchez-Moral, Concepció Violán, ..., Ramon Monfà, Maria-Rosa Sarrias, Pere-Joan Cardona

mrsarrias@igtp.cat (M.-R.S.)
pcardona@germanstrias@gencat.cat (P.-J.C.)

Highlights
Trained immunity (TI) may be an alternative to tackle new SARS-CoV-2 variants

The mycobacterium *Mycobacterium manresensis* (Mm) induced TI in monocytes *in vitro*

Nyaditum resae (NR, containing Mm) did not induce TI in a clinical trial

NR changed the profile of circulating immune cells in a clinical trial

de Homdedeu et al., iScience 26, 106873
June 16, 2023 © 2023 The Authors.
<https://doi.org/10.1016/j.isci.2023.106873>



Article

Mycobacterium manresensis induces trained immunity *in vitro*

Miquel de Homdedeu,^{1,2,3,22} Lidia Sanchez-Moral,^{1,22} Concepció Violán,^{4,5,6,7,8,22} Neus Ràfols,¹ Dan Ouchi,⁴ Berta Martín,⁹ Miguel A. Peinado,⁹ Alhelí Rodríguez-Cortés,¹⁰ Marta Arch-Sisquella,² Daniel Perez-Zsolt,¹¹ Jordana Muñoz-Basagoiti,¹¹ Nuria Izquierdo-Useros,^{11,12} Betlem Salvador,⁴ Joan Matllo,¹³ Sergi López-Serrano,^{14,15,16} Joaquim Segalés,^{14,16,17} Cristina Vilaplana,^{2,3,18,19,21} Pere Torán-Monserrat,^{4,5,6,7} Rosa Morros,⁴ Ramon Monfà,⁴ Maria-Rosa Sarrias,^{1,20,23,*} and Pere-Joan Cardona^{2,3,18,19,*}

SUMMARY

The COVID-19 pandemic posed a global health crisis, with new severe acute respiratory syndrome coronavirus 2 (SARS-CoV-2) variants weakening vaccine-driven protection. Trained immunity could help tackle COVID-19 disease. Our objective was to analyze whether heat-killed *Mycobacterium manresensis* (hkMm), an environmental mycobacterium, induces trained immunity and confers protection against SARS-CoV-2 infection. To this end, THP-1 cells and primary monocytes were trained with hkMm. The increased secretion of tumor necrosis factor alpha (TNF- α), interleukin (IL)-6, IL-1 β , and IL-10, metabolic activity, and changes in epigenetic marks suggested hkMm-induced trained immunity *in vitro*. Healthcare workers at risk of SARS-CoV-2 infection were enrolled into the MANRECOVID19 clinical trial (NCT04452773) and were administered *Nyaditum resae* (NR, containing hkMm) or placebo. No significant differences in monocyte inflammatory responses or the incidence of SARS-CoV-2 infection were found between the groups, although NR modified the profile of circulating immune cell populations. Our results show that *M. manresensis* induces trained immunity *in vitro* but not *in vivo* when orally administered as NR daily for 14 days.

INTRODUCTION

The coronavirus disease 2019 (COVID-19) pandemic, caused by severe acute respiratory syndrome coronavirus 2 (SARS-CoV-2), has led to a global health crisis.¹ As of 27 July 2022, it has affected over 567 million individuals and resulted in over 6.3 million deaths worldwide.² In this context, although several clinical trials have demonstrated promising results on the efficacy, safety, adverse events, and immunogenicity of available vaccines,³ new SARS-CoV-2 variants could evade such protection.^{4–7}

Trained immunity, which comprises the functional reprogramming of innate immune cells (especially monocytes and natural killer [NK] cells), may provide an alternative approach to tackle such variants. Trained immunity is triggered by an initial stimulus, and it leads to an increased response to a second challenge.⁸ Although not fully understood, this functional reprogramming involves epigenetic, metabolic, and transcriptional changes, which together boost the inflammatory and antimicrobial functions of innate immune cells. The bacillus Calmette-Guérin (BCG) vaccine—the live-attenuated vaccine form of a virulent isolate of *Mycobacterium bovis* (a bacterium closely related to *Mycobacterium tuberculosis* [Mtb], which causes tuberculosis [TB])—has been shown to induce trained immunity in monocytes.⁹ BCG vaccination has been routinely implemented in many countries worldwide and has brought about a reduction in TB incidence in children and adults.^{10–12} In addition, BCG immunization was reported to induce protection against other mycobacteria such as *Mycobacterium leprae*¹³ and *Mycobacterium ulcerans*.¹⁴ Interestingly, initial studies showed that it also reduced the incidence of respiratory syncytial virus infection and hospitalization due to respiratory infection and sepsis in children in Guinea-Bissau¹⁵ and Spain,¹⁶ and conferred protection from acute respiratory tract infections in the elderly in Indonesia.¹⁷ More recently, studies have shown that BCG vaccination induces protection in experimental human infection with non-pathogenic,

¹Innate Immunity Group, Germans Trias i Pujol Research Institute (IGTP), 08916 Badalona, Spain

²Experimental Tuberculosis Unit, Germans Trias i Pujol Research Institute (IGTP), 08916 Badalona, Spain

³Department of Genetics and Microbiology, Autonomous University of Barcelona (UAB), 08193 Bellaterra, Spain

⁴Jordi Gol University Research Institute in Primary Care, 08007 Barcelona, Spain

⁵North Metropolitan Research Support Unit, Jordi Gol University Research Institute in Primary Care (IDIAP Jordi Gol), Mataró, Spain

⁶Northern Metropolitan Primary Care Management, Catalan Institute of Health, 08916 Badalona, Spain

⁷Germans Trias i Pujol Research Institute (IGTP), 08916 Badalona, Spain

⁸Autonomous University of Barcelona (UAB), 08193 Bellaterra, Spain

⁹Program of Predictive and Personalized Medicine of Cancer, Germans Trias i Pujol Research Institute (PMPPC-IGTP), 08916 Badalona, Spain

¹⁰Department of Pharmacology, Toxicology, and Therapeutics, Veterinary Faculty, Autonomous University of Barcelona, 08193 Bellaterra, Spain

¹¹IrsiCaixa AIDS Research Institute, 08916 Badalona, Spain

¹²Centre for Biomedical Research on Infectious Diseases (CIBERINFEC), Madrid, Spain

¹³Department of Prevention and Risks, Germans Trias i

Continued



live-attenuated yellow fever vaccine virus¹⁸ and enhances immune responses to influenza vaccination,¹⁹ thereby providing direct evidence of the broad protection conferred by this vaccination. Additionally, BCG vaccination was found to alter some of the clinical, immunological, and parasitological outcomes of malaria infection in a subset of volunteers in a controlled human malaria infection clinical trial.²⁰

Regarding COVID-19, since BCG was previously reported to protect against viral respiratory infections in the elderly,^{17,21} over 30 clinical trials have been registered to determine whether BCG vaccination can protect against COVID-19.²² Among these trials, results from A randomized Clinical Trial for enhanced trained Immune responses through BCG vaccination to prevent Infections by COVID-19 (ACTIVATE-2) suggest that BCG vaccination confers some protection against COVID-19 to patients with comorbidities who are older than 50.²³ Additionally, clinical trials specifically involving healthcare workers (HCWs) have been performed, with the aim of ensuring patient care throughout the pandemic.^{24–30} Although no significant efficacy has yet been proven in HCWs,^{27–30} the BCG Vaccination to Reduce the Impact of COVID-19 in Healthcare Workers (BRACE) trial indicated that BCG vaccination, but not placebo vaccination, modifies key immunological parameters associated with severe COVID-19—findings that are consistent with a protective immune response.³¹

Nyaditum resae (NR) is a food supplement comprising heat-killed *Mycobacterium manresensis* (hkMm). *M. manresensis* is an environmental mycobacterium that belongs to the *Mycobacterium fortuitum* complex.³² NR has been shown to halt progression to active TB by increasing memory-specific T regulatory (Treg) cells and interleukin (IL)-10 and reducing neutrophilic infiltration, as well as tumor necrosis factor alpha (TNF- α), interferon (IFN) γ , IL-6, and IL-17 production in the lungs.^{33,34} This mycobacterium also induces a specific increase in the response of Treg cells, including memory cells *in vitro*, and it shows an excellent safety profile in humans.³⁵ Thus, treatment with *M. manresensis* may provide a potential approach to reduce the severity of COVID-19. Furthermore, *M. bovis*, which is present in the BCG vaccine, and *M. manresensis* are mycobacteria with a similar cell wall, built mainly on mycolic acids and that contains a substantial proportion of trehalose dimycolate (TDM).³⁶ Molecules like TDM have been identified as potent immunomodulators, conferring significant heterologous resistance against infections, such as influenza virus.³⁷ Therefore, we hypothesized that hkMm may also induce trained immunity and show an improved safety profile with respect to BCG and may therefore have the capacity to contribute to the management of the COVID-19 pandemic.

Here we addressed whether hkMm induces trained immunity *in vitro* and *in vivo* and assessed the impact of oral uptake of NR on SARS-CoV-2 infection and the course of COVID-19 disease (namely, incidence, severity, and absenteeism caused by the disease) in a cohort of highly exposed HCWs in Spain.

RESULTS

hkMm induces trained immunity in the human monocytic THP-1 cell line

The human monocytic THP-1 cell line has been widely used to model the function and regulation of human primary macrophages. Here we sought to establish a protocol of trained immunity in the THP-1 cell line using heat-killed BCG (hkBCG) and test whether hkMm was also capable of inducing an equivalent response. To this end, we examined two hallmarks of trained immunity, namely enhanced inflammatory secretion and shift of macrophage metabolism toward glycolysis. The standardized protocol is shown in Figure 1A. Initial priming of the macrophages with hkBCG or hkMm led to higher TNF- α , IL-6, and IL-1 β expression than in untrained cells when they were exposed to lipopolysaccharides (LPS) as secondary stimulus ($p = 0.0313$, Figure 1B). Likewise, higher levels of TNF- α and IL-1 β were observed when cells were challenged with heat-killed *Staphylococcus aureus* (hk *S. aureus*) and inactivated (In) SARS-CoV-2, respectively ($p = 0.0313$, Figures 1C and 1D). In contrast, no differences were detected in IL-6 or IL-1 β production when cells were rechallenged with hk *S. aureus*, in TNF- α or IL-6 production when cells were rechallenged with InSARS-CoV-2, or in TNF- α , IL-6, or IL-1 β production after cells were stimulated with heat-killed *M. tuberculosis* (hkMtb) and In swine influenza virus (SIV) H1N1 (data not shown). Regarding metabolic activity, hkBCG- and hkMm-trained THP-1 cells showed increased levels of L(+)-Lactate ($p = 0.0313$, Figure 1E), although at this time point no differences in the expression of glycolytic enzymes were detected (Figure S1A). Taken together, these results suggest that hkMm induces trained immunity *in vitro* in THP-1 cells to the same extent as hkBCG. Furthermore, it is remarkable that when analyzing cell size, hkBCG- and hkMm-trained THP-1 cells appeared to be larger than untrained cells ($p = 0.0152$ and $p = 0.0087$, respectively Figure S1B)—an effect that was previously observed for β -glucan and BCG training.³⁸

Pujol University Hospital, Northern Metropolitan Territorial Management, Catalan Health Institute, 08916 Badalona, Spain

¹⁴Joint IRTA-UAB Research Unit in Animal Health, Animal Health Research Center (CReSA), Autonomous University of Barcelona (UAB), 08193 Bellaterra, Spain

¹⁵Institute of Agrifood Research and Technology, Animal Health Program, Animal Health Research Center (CReSA), Autonomous University of Barcelona (UAB), 08193 Bellaterra, Spain

¹⁶OIE Collaborating Centre for the Research and Control of Emerging and Re-Emerging Swine Diseases in Europe (IRTA-CReSA), 08193 Bellaterra, Spain

¹⁷Department of Animal Health and Anatomy, Faculty of Veterinary Medicine, Autonomous University of Barcelona (UAB), 08193 Bellaterra, Spain

¹⁸Centre for Biomedical Research on Respiratory Diseases (CIBERES), Madrid, Spain

¹⁹Microbiology Department, Laboratori Clínic Metropolitana Nord, Germans Trias i Pujol University Hospital, 08916 Badalona, Spain

²⁰Centre for Biomedical Research on Liver and Digestive Diseases (CIBEREHD), Madrid, Spain

²¹Direcció Clínica Territorial de Malalties Infeccioses i Salut Internacional de Gerència Territorial Metropolitana Nord, Barcelona, Spain

²²These authors contributed equally

²³Lead contact

*Correspondence: mrsarrias@igtp.cat (M.-R.S.), pcardonai.germanstrias@gencat.cat (P.-J.C.)

<https://doi.org/10.1016/j.isci.2023.106873>

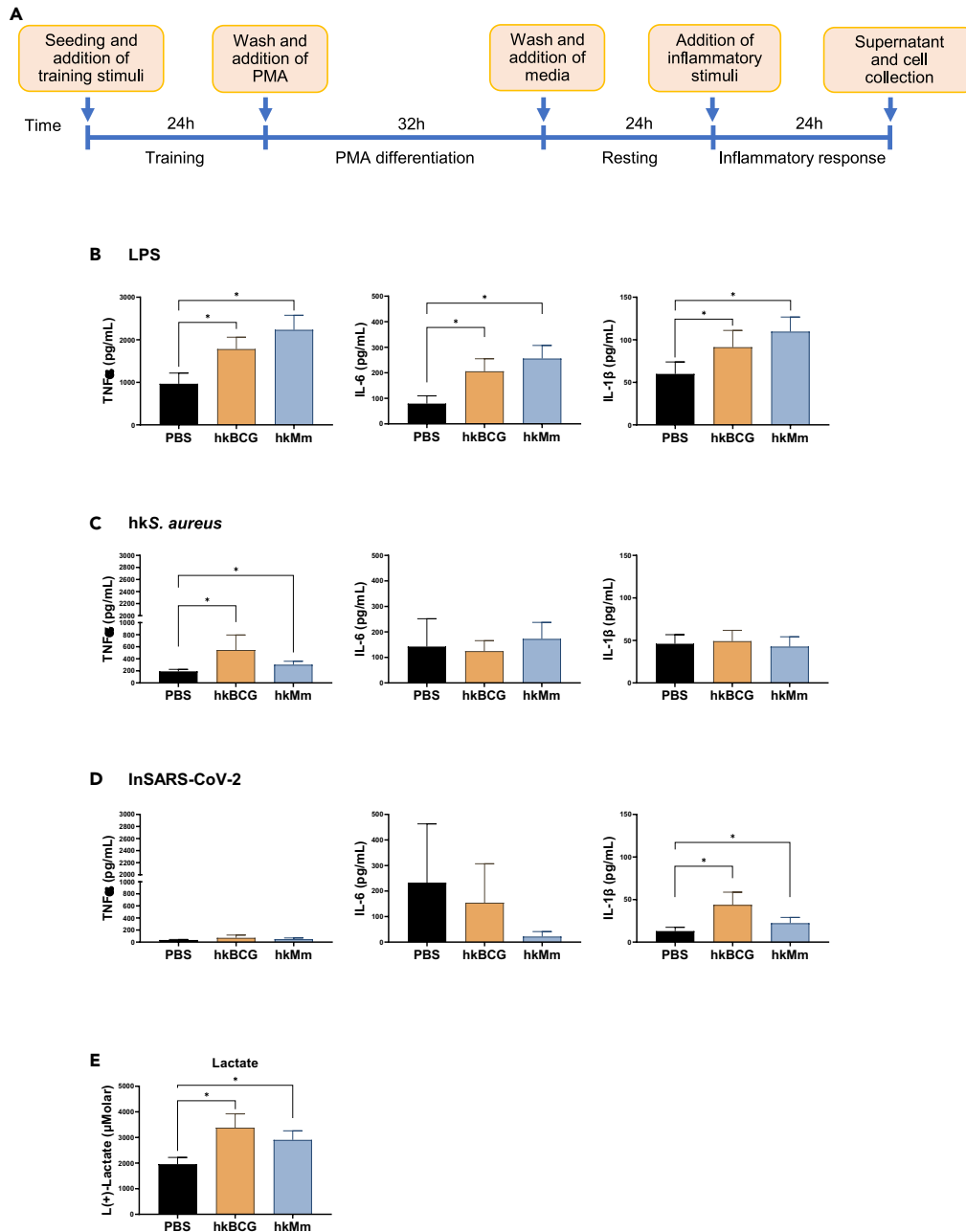


Figure 1. Increased inflammatory responses of THP-1 cells upon heat-killed *M. manresensis* training

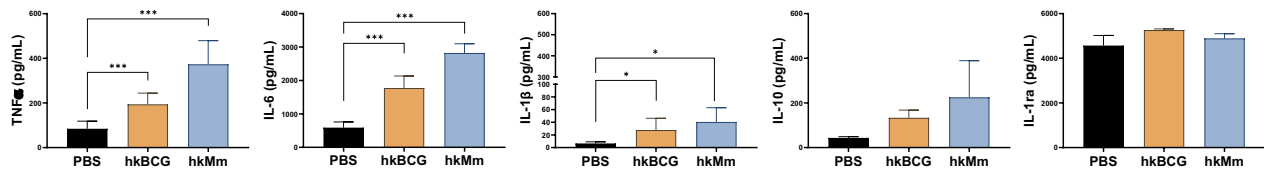
(A) Schematic overview of trained immunity methodology in THP-1 cells. Production of cytokines after training and the secondary stimulation with (B) 10 ng/mL LPS, (C) 5×10^6 cfu/mL *hkS. aureus*, and (D) 0.218 ng nucleocapsid/mL InSARS-CoV-2.

(E) Levels of L(+)-Lactate in untrained (PBS) and hkBCG- and hkMm-trained monocytes. ($n = 6$, $*p < 0.05$, Wilcoxon matched-pairs signed-rank test, mean \pm SEM). hkMm, heat-killed *M. manresensis*; hkBCG, heat-killed BCG; *hkS. aureus*, heat-killed *S. aureus*; InSARS-CoV-2, inactivated SARS-CoV-2.

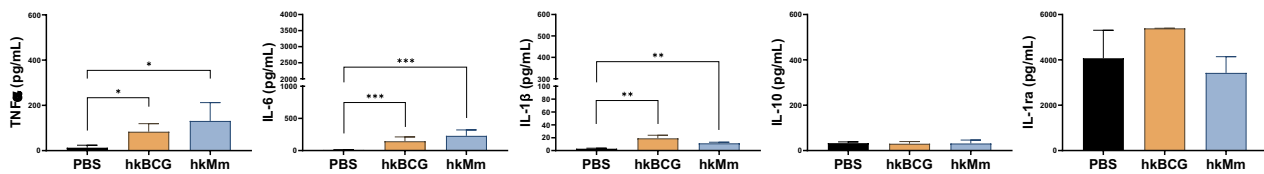
hkMm induces trained immunity in human primary monocytes

After confirming the capacity of *M. manresensis* to induce trained immunity *in vitro* in the monocyte-like THP-1 cell line, we tested whether it could also induce trained immunity in primary monocytes. Like hkBCG training, hkMm enhanced TNF- α , IL-6, and IL-1 β production as compared to the control when monocytes

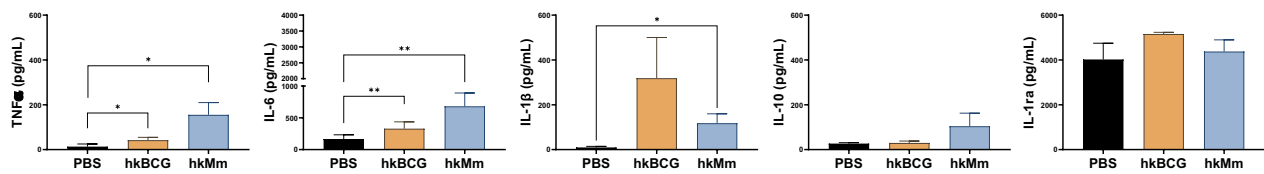
A LPS



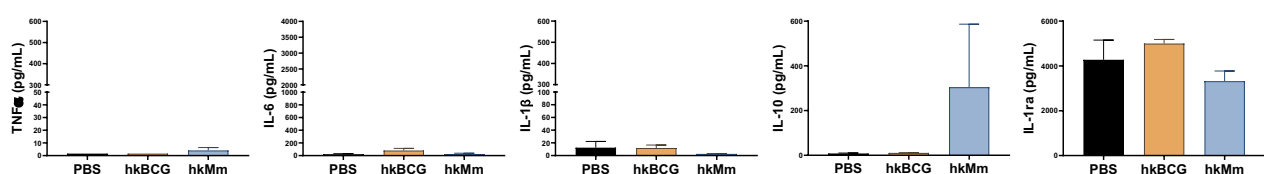
B *hkS. aureus*



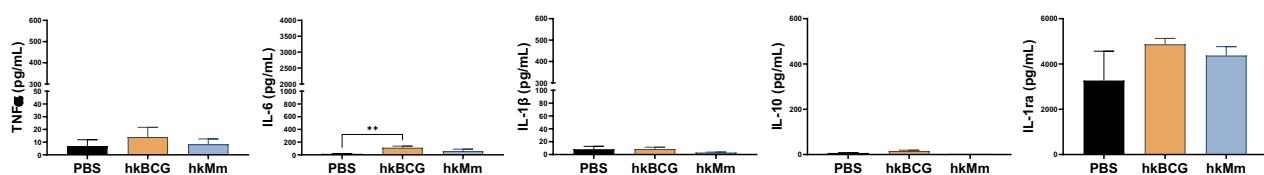
C *hkMtb*



D InSARS-CoV-2



E InSIV H1N1



F Lactate

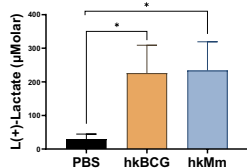


Figure 2. Increased cytokine responses of primary monocytes upon heat-killed *M. manresensis* training

(A–E) Cytokines from the supernatant of cultured trained monocytes were measured by ELISA after the secondary stimulation with (A) 10 ng/mL LPS, (B) 5×10^6 cfu/mL *hkS. aureus*, (C) 10^6 cfu/mL *hkMtb*, (D) 0.218 ng nucleocapsid/mL InSARS-CoV-2, and (E) $10^{4.29}$ TCID₅₀/mL InSIV H1N1.

(F) Levels of L(+)-Lactate in untrained (PBS) and *hkBCG*- and *hkMm*-trained primary monocytes. ($n = 5-11$, $*p < 0.05$, $**p < 0.01$, $***p < 0.001$, Wilcoxon matched-pairs signed-rank test, mean \pm SEM; Spearman's ρ and p values are shown in the right corner of the correlation plot. *hkMm*, heat-killed *M. manresensis*; *hkBCG*, heat-killed *B. cereus*; *hkS. aureus*, heat-killed *S. aureus*; *hkMtb*, heat-killed *M. tuberculosis*; InSARS-CoV-2, inactivated SARS-CoV-2; InSIV H1N1, inactivated SIV H1N1.

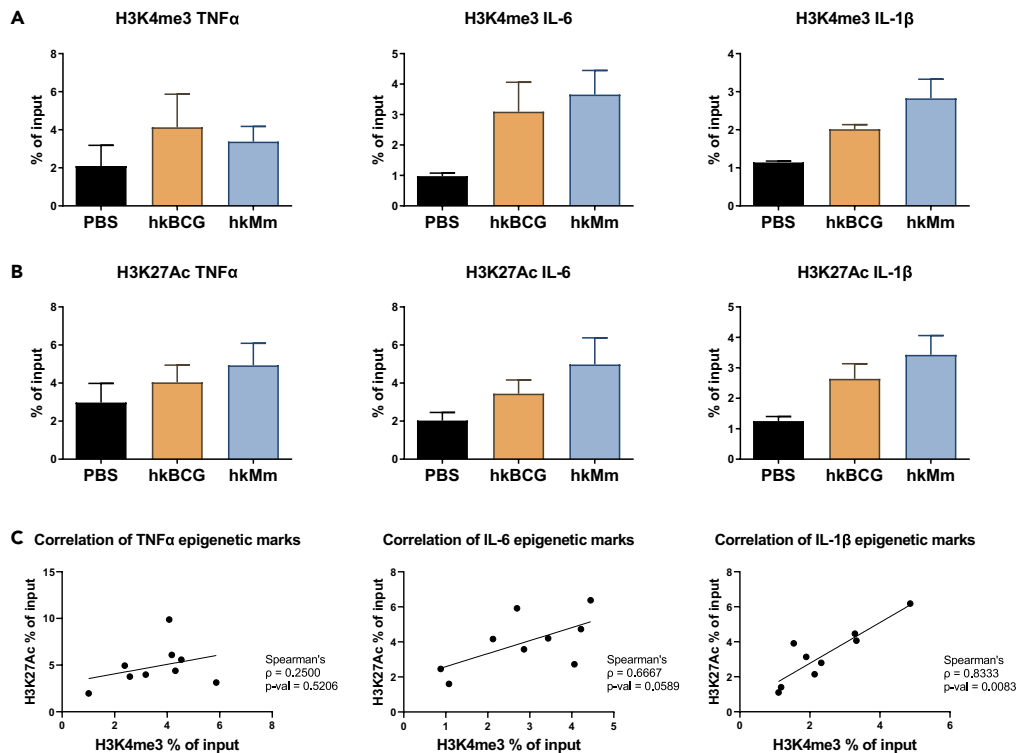


Figure 3. Trained immunity by heat-killed *M. manresensis* generates epigenetic modifications

(A and B) Enrichment in (A) H3K4me3 and (B) H3K27ac in TNF- α , IL-6, and IL-1 β gene promoters in untrained and hkBCG- and hkMm-trained primary monocytes. Results are reported as enrichment of immunoprecipitated DNA relative to the input (n = 3, Wilcoxon matched-pairs signed-rank test, mean \pm SEM).

(C) Correlation between H3K4me3 and H3K27ac epigenetic modifications in TNF- α , IL-6, and IL-1 β gene promoters.

(Spearman's ρ and p values are shown in the right corner of the plot). hkMm, heat-killed *M. manresensis*; hkBCG, heat-killed BCG.

were exposed to LPS (p = 0.001, p = 0.001, and p = 0.0156, respectively, Figure 2A) and hk*S. aureus* (p = 0.0313, p = 0.001, and p = 0.0078, respectively, Figure 2B) as inflammatory stimuli. In addition, hkMm-trained monocytes showed greater TNF- α and IL-6 production when challenged with hkMtb as secondary stimulus (p = 0.0313 and p = 0.0078, Figure 2C). However, stimulation with InSARS-CoV-2 and InSIV H1N1 had no effect on TNF- α , IL-6, and IL-1 β production after the initial priming with hkBCG or hkMm (Figures 2D and 2E). hkMm-trained primary monocytes rechallenged with LPS, hkMtb, and InSARS-CoV-2 showed an increase in the production of IL-10, although this increase was not significant (Figures 2A–2E). Regarding IL-1Ra, no differences were detected in its production by either hkBCG- or hkMm-trained primary monocytes (Figures 2A–2E). With respect to metabolic activity, hkBCG- and hkMm-trained human monocytes increased L(+)-Lactate production (p = 0.0156, Figure 2F). Taken together, these results indicate that hkMm induces trained immunity in human primary monocytes *in vitro* by boosting metabolic functions and inflammatory responses against LPS, hk*S. aureus*, and hkMtb.

hkMm induces epigenetic modifications in human monocytes

Next, we analyzed the epigenetic marks of TNF- α , IL-6, and IL-1 β gene promoters, which have been proposed as key elements mediating long-term enhanced responses in trained immunity with BCG.³⁹ We applied chromatin immunoprecipitation (ChIP) to study the histone modifications associated with open/active chromatin, such as trimethylation of histone H3 at lysine 4 (H3K4me3) and acetylation of histone H3 at lysine 27 (H3K27ac). Increased H3K4me3 and H3K27ac levels were found in the promoter regions of TNF- α , IL-6, and IL-1 β in primary monocytes trained with hkMm (Figures 3A and 3B, respectively). These observations suggest that chromatin is more active in the promoter regions of proinflammatory genes, thus leading to an increased expression and responsiveness to secondary stimuli.

Table 1. Baseline characteristics of enrolled participants

	Overall	Placebo	Nyaditum resae®	p value
N (%)	317	103	214	
Sex				
Male	68 (21.5)	17 (16.5)	51 (23.8)	0.179
Female	249 (78.5)	86 (83.5)	163 (76.2)	
Age (mean (SD)), years	45.31 (11.30)	45.93 (11.95)	45.01 (10.99)	0.499
Weight (mean (SD)), kg	69.64 (14.63)	68.83 (14.27)	70.03 (14.82)	0.494
Height (mean (SD)), cm	165.07 (9.03)	164.22 (8.69)	165.47 (9.18)	0.249
BMI (mean (SD)), kg/m ²	25.50 (4.69)	25.50 (4.90)	25.50 (4.59)	0.997
Smoker status				
Smoker	93 (29.3)	33 (32.0)	60 (28.0)	0.751
Ex-smoker	53 (16.7)	16 (15.5)	37 (17.3)	
Non-smoker	171 (53.9)	54 (52.4)	117 (54.7)	
Comorbidities				
No	172 (54.3)	55 (53.4)	117 (54.7)	0.926
Yes	145 (45.7)	48 (46.6)	97 (45.3)	
Number of comorbidities				
0	172 (54.3)	55 (53.4)	117 (54.7)	0.830
1	39 (12.3)	16 (15.5)	23 (10.7)	
2	83 (26.2)	26 (25.2)	57 (26.6)	
3	18 (5.7)	5 (4.9)	13 (6.1)	
4	4 (1.3)	1 (1.0)	3 (1.4)	
5	1 (0.3)	0 (0.0)	1 (0.5)	
Respiratory diseases				
Asthma	28 (8.8)	9 (8.7)	19 (8.9)	1.000
COPD	1 (0.3)	1 (1.0)	0 (0.0)	0.708
Other respiratory diseases	5 (1.6)	4 (3.9)	1 (0.4)	0.071
Cardiovascular diseases				
Hypertension	24 (7.6)	6 (5.8)	18 (8.4)	0.556
Other cardiovascular comorbidities ^a	8 (2.5)	4 (3.9)	4 (1.9)	0.491
Diabetes	5 (1.6)	2 (1.9)	3 (1.4)	1.000
Dyslipidaemia	14 (4.4)	4 (3.9)	10 (4.7)	0.977
Thyroid disorders	26 (8.2)	7 (6.8)	19 (8.9)	0.679

BMI, body mass index. SD, standard deviation. COPD, chronic obstructive pulmonary disease.

^aOther cardiovascular comorbidities: atrial fibrillation, other arrhythmias, myocardial infarction.

Moreover, H3K4me3 and H3K27ac levels were highly correlated for the IL-1 β gene promoter (p value = 0.0083, ρ = 0.8333, [Figure 3C](#)), thus emphasizing the role of IL-1 β in trained immunity. Overall, these results suggest that *in vitro* training with hkMm increases H3K4me3 and H3K27ac at the promoter sites of proinflammatory genes.

Oral administration of hkMm does not influence SARS-CoV-2 infection

The MANRECOVID19 clinical trial included 317 participants, of which 214 were in the NR group and 103 in the placebo group. The demographics and baseline characteristics of the participants are described in [Table 1](#), and the professional categories of the HCWs who participated in the study are described in [Table S2](#). A full description of participants is given in the flowchart in [Figure 4](#). The main variable to assess efficacy was the cumulative incidence of documented SARS-CoV-2 infection, as determined by RT-PCR, rapid antigenic test (RAT), or serological blood test. The study procedures and variables collected at each visit are listed in [Table S3](#). All participants who met inclusion criteria were studied as “intention to treat” (ITT) population. The

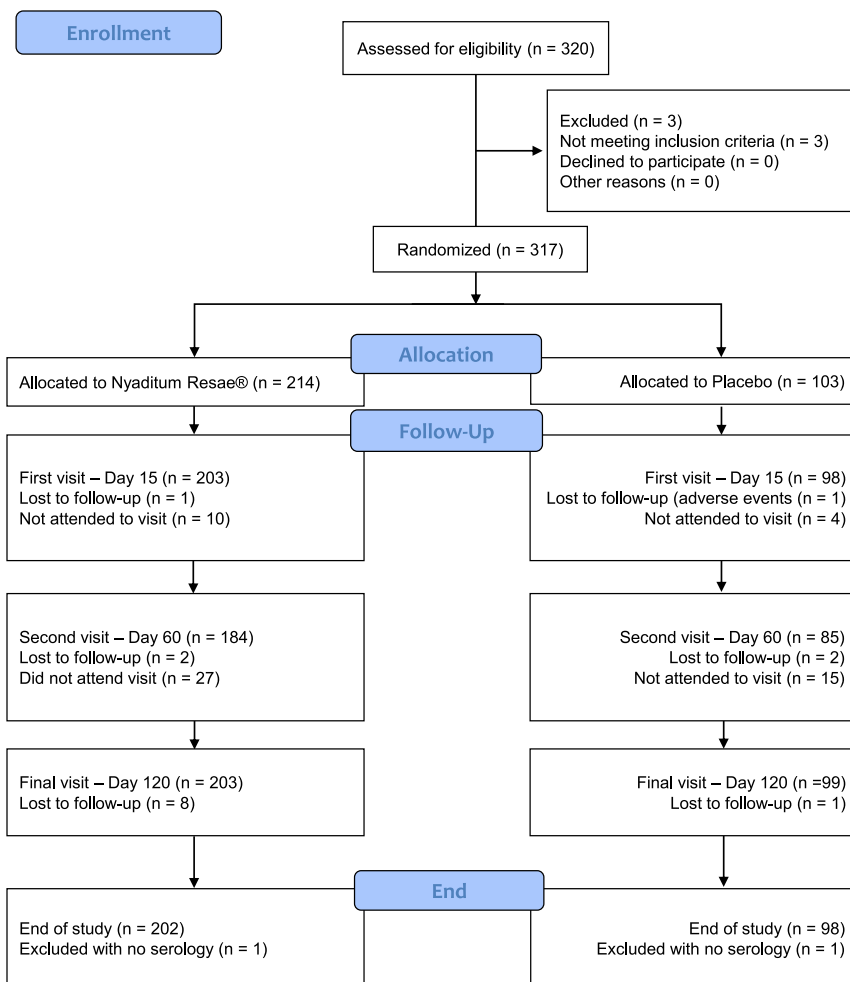


Figure 4. Flowchart of study participants

A total of 320 individuals were assessed for eligibility to participate in the study; 317 were randomized to receive Nyaditum resae (n = 214) or placebo (n = 103), and they composed the ITT sample. The PP sample was composed of 198 participants, 131 in the Nyaditum resae group and 67 in the placebo group.

“per protocol” (PP) population was composed of those participants with a confirmed negative result in the SARS-CoV-2 test before the start of the study who completed the final study visit without significant deviations from the protocol and had not received a COVID-19 vaccine before the end of the study. In the ITT population, 62 (19.6%) of the tests conducted were positive (Table S4), while 21 (10.6%) were positive in the PP population (Table S5). We found no significant differences in the positivity of the tests between the two treatment groups. Tables S6 and S7 show the type of tests conducted and the vaccinations of the ITT and the PP populations, respectively. The cumulative incidence of SARS-CoV-2 infection did not differ between the two treatment arms for the ITT population (Figure 5A), as shown in the logistic regression model (odds ratio [OR] 1.22, 95% confidence interval [CI] 0.64–2.35) (Table S6). Women had a lower incidence of infection than men (OR 0.96, 95% CI 0.94–0.99). A higher number of comorbidities were associated with a higher incidence of infection (OR 1.54, 95% CI 1.05–2.25). Previous vaccination (seasonal influenza and/or pneumococcal vaccine) was also associated with a higher risk of SARS-CoV-2 infection (OR 7.04, 95% CI 3.11–15.93). Receiving a comedication at baseline was associated with a lower incidence of infection (OR 0.25, 95% CI 0.1–0.6). The rest of the variables showed no statistical significance. For the PP sample, we did not find differences in the incidence of SARS-CoV-2 infection between the NR and placebo groups (Figure 5B) (OR 2.03, 95% CI 0.62–6.67, Table S7). Women had a lower incidence of infection than men (OR 0.27, 95% CI 0.09–0.77). A higher BMI and previous seasonal influenza and/or pneumococcal vaccine were associated with a higher risk of SARS-CoV-2 (OR 1.15, 95% CI 1.03–1.30 and OR 8.28, 95% CI 2.62–26.11, respectively).

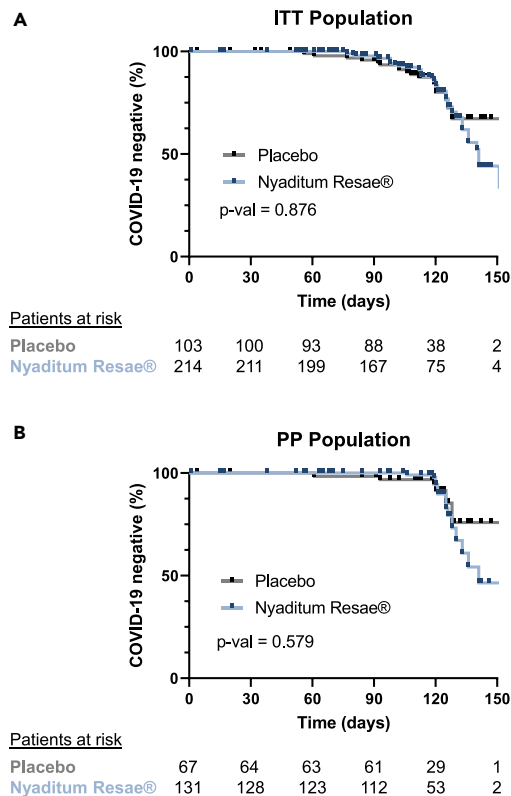


Figure 5. Heat-killed *M. manresensis* does not protect against SARS-CoV-2 infection

(A and B) Kaplan-Meier curves and patients at risk data for the time to COVID-19 infection in each treatment arm for the (A) ITT and the (B) PP population. Follow-up days truncated at 150, but there are patients with up to 175 days of follow-up.

Oral administration of hkMm does not modify the inflammatory responses of peripheral blood monocytes

Given that hkMm induced trained immunity *in vitro*, we examined whether oral uptake of NR for 14 days had any effect on the inflammatory responses of circulating monocytes. To this end, peripheral blood was collected from a subset of healthy volunteers also included in the MANRECOVID19 clinical trial. Of the 63 volunteers recruited, 6 were lost, resulting in a final population of 57 participants, who were divided into the placebo ($n = 18$) and NR ($n = 39$) experimental groups. The demographic characteristics of the volunteers are listed in Table 2. Peripheral blood mononuclear cells (PBMCs) were isolated on day 0 and day 15 after intervention and challenged with an array of stimuli, namely LPS, hkMtb, hk*S. aureus*, InSARS-CoV-2, and InSIV H1N1 viral particles, and their inflammatory responses were determined. After fold change (FC) comparison, the results showed no changes in proinflammatory cytokines (Figure 6) from baseline to day 15, when comparing the NR group with the placebo group. However, of note, reduced IL-1 β levels were observed in response to hkMtb, InSARS-CoV-2, and InSIV H1N1, although these differences were not significant. Raw differences in the cytokine levels are shown in Table S8. Taken together, these results indicate that the oral administration of hkMm does not modify inflammatory responses of circulating monocytes *in vivo*.

Oral administration of hkMm changes the profile of circulating immune cell populations

Finally, we studied whether oral administration of hkMm had a direct effect on the frequency of circulating leukocytes. To this end, we stained PBMCs from both visits for spectral flow cytometry analysis using the gating strategy shown in Figure S2. The analysis showed that total lymphocytes remained alike between groups (Figure 7A), as did B cells (CD3⁻, CD19⁺) (Figure 7B), T cells (CD3⁺) (Figure 7C), CD8⁺ T cells (Figure 7D), and CD4⁺ T cells (Figure 7E). Interestingly, activated CD4⁺ T cells (CD4⁺CD25⁺ T cells) were increased in the NR group (Fold change (FC) of 0.93 [0.90, 1.01] vs. 1.04 [0.97, 1.11], $p = 0.017$, Figure 7F). Regarding Treg cells (CD4⁺CD25⁺CD127^{lo}), an upward trend was noticed in the NR group, although this

Table 2. Demographic characteristics of the healthy volunteers used in trained immunity assessment

	Total	Placebo	Nyaditum resae®	p value
N	57	18	39	
Gender (%)				
Male	11 (19.3)	4 (22.2)	7 (17.9)	0.985
Female	46 (80.7)	14 (77.8)	32 (82.1)	
Age (mean (SD))	45.39 (11.70)	49.61 (12.05)	43.44 (11.15)	0.063
Smoking habit (%)				
Smoker	17 (29.8)	6 (33.3)	11 (28.2)	0.218
Ex-smoker	7 (12.3)	4 (22.2)	3 (7.7)	
Non-smoker	33 (57.9)	8 (44.4)	25 (64.1)	
Professional (%)				
Management and services technician	5 (8.8)	4 (22.2)	1 (2.6)	0.102
Patient care technicians	15 (26.3)	4 (22.2)	11 (28.2)	
Graduate Nurse	28 (49.1)	7 (38.9)	21 (53.8)	
Primary Care Physician	4 (7.0)	1 (5.6)	3 (7.7)	
Hospital Care Physician	1 (1.8)	1 (5.6)	0 (0.0)	
Caretaker	1 (1.8)	1 (5.6)	0 (0.0)	
Physiotherapist	2 (3.5)	0 (0.0)	2 (5.1)	
Other	1 (1.8)	0 (0.0)	1 (2.6)	
Grouped professional (%)				
Nurse	43 (75.4)	11 (61.1)	32 (82.1)	0.195
Physician	5 (8.8)	2 (11.1)	3 (7.7)	
Other	9 (15.8)	5 (27.8)	4 (10.3)	
Adherence to treatment (%)				
No	2 (3.5)	1 (5.6)	1 (2.6)	1
Yes	55 (96.5)	17 (94.4)	38 (97.4)	
Adverse event (%)				
No	47 (82.5)	15 (83.3)	32 (82.1)	1
Yes	10 (17.5)	3 (16.7)	7 (17.9)	
Comorbidities (%)				
No	31 (54.4)	10 (55.6)	21 (53.8)	1
Yes	26 (45.6)	8 (44.4)	18 (46.2)	
Heart disease (%)				
No	52 (91.2)	16 (88.9)	36 (92.3)	1
Yes	5 (8.8)	2 (11.1)	3 (7.7)	
Respiratory disease (%)				
No	52 (91.2)	14 (77.8)	38 (97.4)	0.053
Yes	5 (8.8)	4 (22.2)	1 (2.6)	

SD, standard deviation.

did not reach significance (FC of 0.94 [0.87, 1.03] vs. 1.01 [0.87, 1.12], $p = 0.546$, [Figure 7G](#)). In contrast, no changes were observed in total NK cells ([Figure 7H](#)) and their subtypes, namely $CD56^+CD16^-$ NKs, $CD56^+CD16^+$ NKs, $CD56^-CD16^+$ NKs ([Figures 7I–7K](#)), and neutrophils ([Figure 7L](#)). As regards monocytes, the number of the total monocytic population experienced a non-significant increase (FC of 1.03 [0.83, 1.38] vs. 1.28 [0.88, 1.68], $p = 0.505$, [Figure 7M](#)). When assessing the different subsets of monocytes, total monocytes, classical ($CD14^{++}$, $CD16^-$) monocytes, and intermediate ($CD14^{++}$, $CD16^+$) monocytes did not present significant alterations ([Figures 7M–7O](#), respectively). However, non-classical monocytes ($CD14^+$, $CD16^{++}$) were significantly increased in the NR group (FC of 0.84 [0.66, 1.32] vs. 1.33 [0.96, 3.45], $p =$

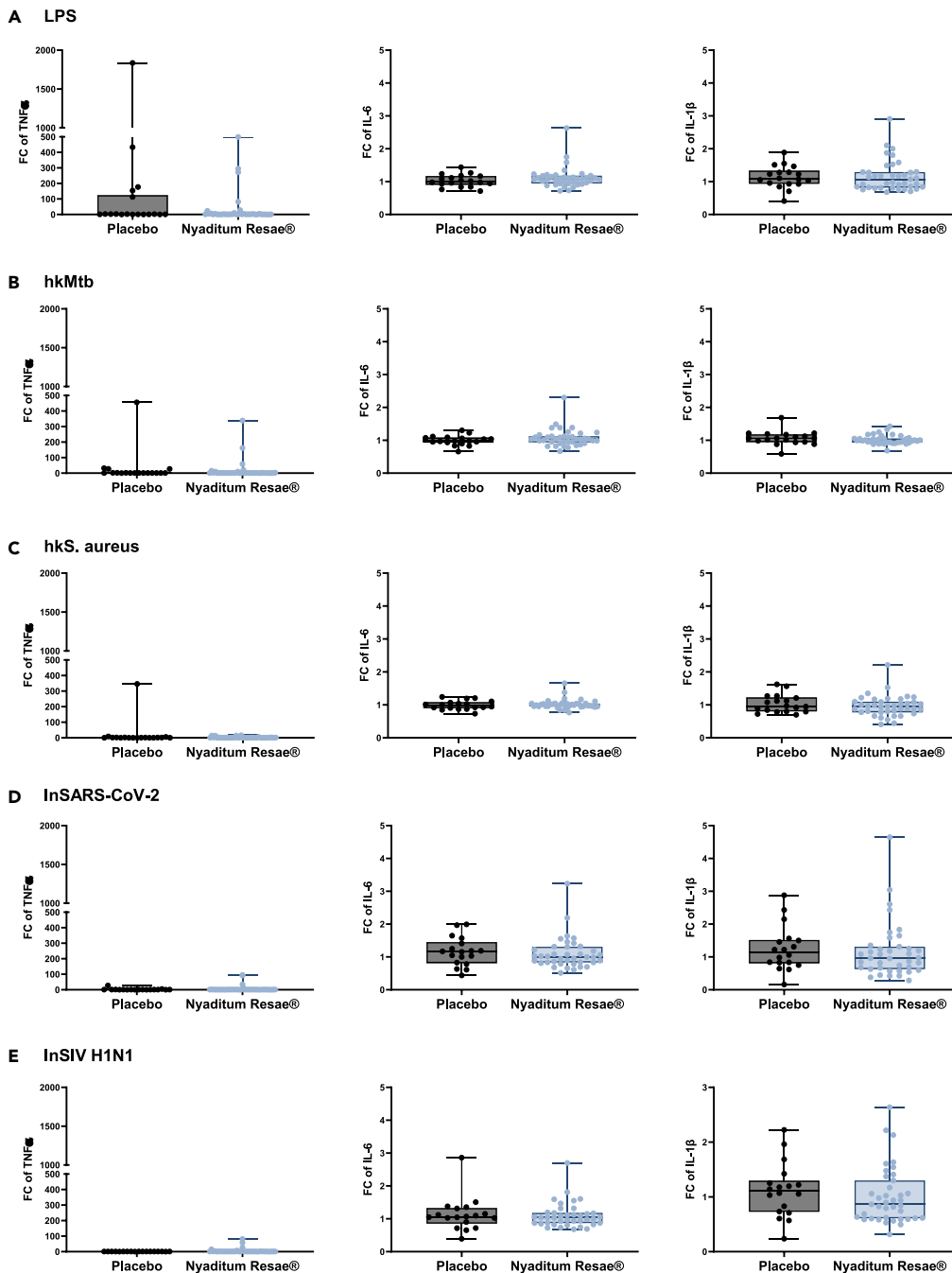


Figure 6. Heat-killed *M. manresensis* does not modify the inflammatory responses of monocytes from healthy volunteers

(A–E) Fold change of TNF- α , IL-6, and IL-1 β after stimulating with (A) 100 ng/mL LPS, (B) 10^6 cfu/mL hkMtb, (C) 10^7 cfu/mL hkS. aureus, (D) 22.5 pfu/mL InSARS-CoV-2, or (E) $10^{3.99}$ TCID₅₀/mL InSIV H1N1 (day 15/day 0). (n = 57, n = 18 Placebo, n = 39 Nyaditum resae, Wilcoxon Mann-Whitney test, boxplot shows the median, quartiles, and minimum and maximum values). Raw data are detailed in Table S8 hkMtb, heat-killed *M. tuberculosis*; hkS. aureus, heat-killed *S. aureus*; InSARS-CoV-2, inactivated SARS-CoV-2; InSIV H1N1, inactivated SIV H1N1.

0.045, Figure 7P). This increase in non-classical monocytes could be due to a reduction in CD16⁺CD14⁻ cells, which are suspected to be dendritic cells.⁴⁰ However, no differences were observed between treatment arms (Figure 7Q). These analyses were performed using a FC comparison of the two visits.

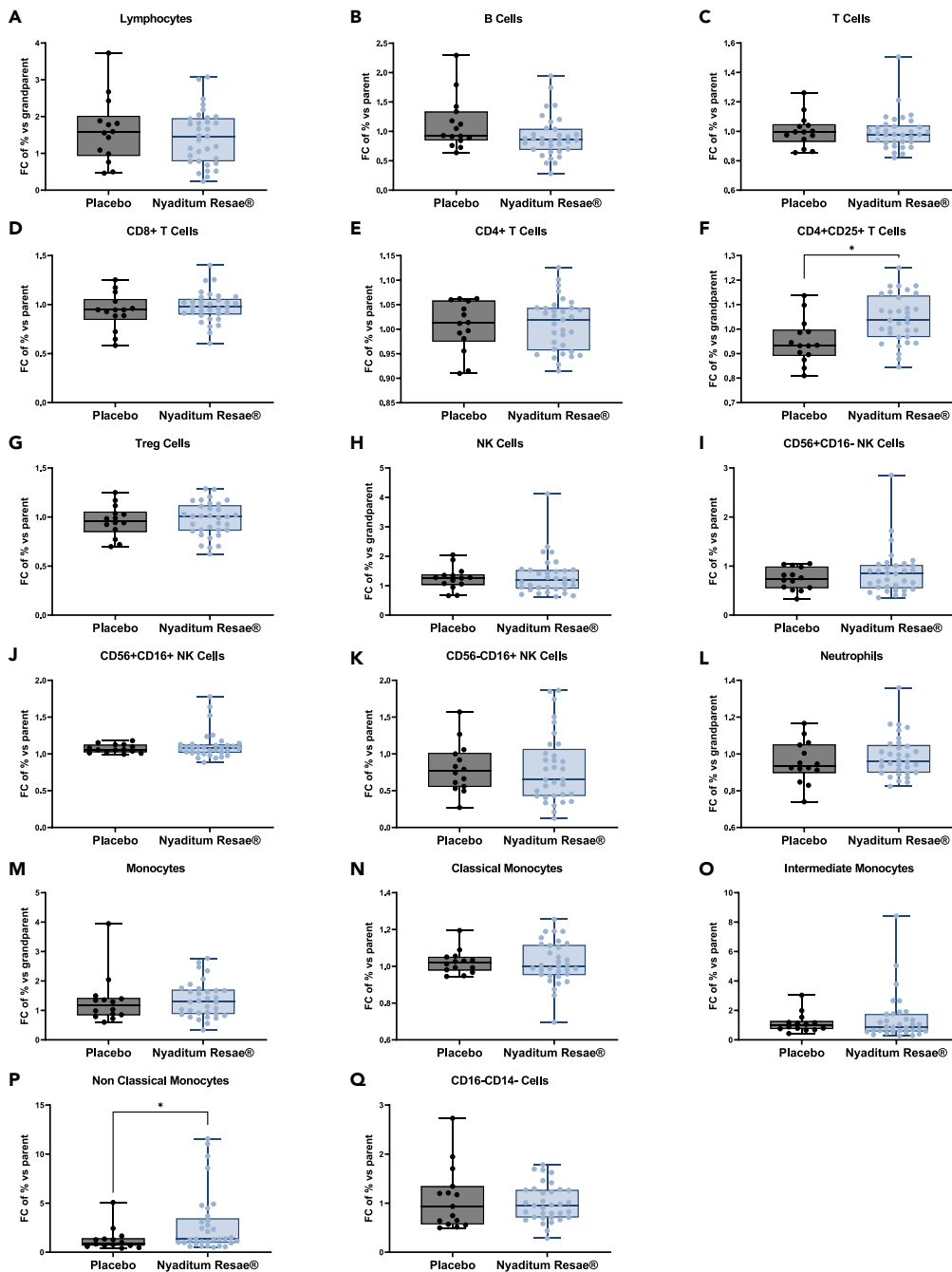


Figure 7. Heat-killed *M. manresensis* changes the profile of circulating immune cell populations from healthy volunteers

(A–Q) Cell populations were analyzed at baseline and 15 days post-treatment administration, and the corresponding fold change (FC) was calculated. Fold change of the frequency of (A) lymphocytes, (B) B cells, (C) T cells, (D) CD8⁺ T cells, (E) CD4⁺ T cells, (F) CD4⁺CD25⁺ T cells, (G) Treg cells, (H) NK cells, (I) CD56⁺CD16⁻ NK cells, (J) CD56⁺CD16⁺ NK cells, (K) CD56⁻CD16⁺ NK cells, (L) neutrophils, (M) monocytes, (N) classical monocytes, (O) intermediate monocytes, (P) non-classical monocytes, and (Q) CD16⁻CD14⁻ cells (day 15/day 0), (n = 57, n = 18 Placebo, n = 39 Nyaditum resae, Wilcoxon Mann-Whitney test, boxplot shows the median, quartiles, and minimum and maximum values). Raw data are detailed in Table S9.

The raw frequencies of all the populations are shown in [Table S9](#). We also studied whether monocytes changed their expression levels of HLA-DR by oral administration of NR, as previous studies have shown that trained immunity increases the expression of antigen-presentation molecules.^{41–43} In flow cytometry, no significant changes were observed in the expression of HLA-DR in monocytes ([Figure S3](#)). Taken together, these results indicate that the oral administration of hkMm significantly modifies the frequency of non-classical monocytes, as well as that of CD4⁺CD25⁺ T cells among circulating leukocytes.

DISCUSSION

Here we present a thorough study assessing whether, like BCG, the environmental mycobacteria species *M. manresensis* induces trained immunity and whether this capacity could find clinical applications in the context of the COVID-19 pandemic.

Indeed, the results from our *in vitro* experiments showed that hkMm induced trained immunity by generating metabolic and epigenetic changes in monocytes, which led to increased inflammatory responses after a set of inflammatory stimuli. Of note, for these experiments we used hkMm instead of NR, since the NR capsule contains mannitol as excipient, which hinders *in vitro* experimentation. More specifically, experiments using the THP-1 cell line revealed that hkMm increased the expression of the following: TNF- α , IL-6, and IL-1 β when these cells were rechallenged with LPS; TNF- α when cells were rechallenged with *hkS. aureus*; and IL-6 when InSARS-CoV-2 was added to the cells. Similarly, when primary monocytes were exposed to LPS, *hkS. aureus*, and hkMtb, hkMm boosted metabolic and inflammatory functions, increasing TNF- α , IL-6, and IL-1 β production, as compared to controls. Regarding anti-inflammatory IL-10 and IL-1Ra, previous studies showed enhanced IL-10 production in trained immunity with β -glucan^{38,44,45} and adenoviral vector COVID-19 vaccine.⁴³ Accordingly, we observed increased responses of hkMm-trained cells when these were stimulated with LPS, hkMtb, and InSARS-CoV-2, although these responses were not significant. Likewise, hkBCG did not alter IL-10 levels—an observation that is consistent with the findings of Bekkering et al.³⁸ Taken together, these results suggest that IL-10 responses after trained immunity may be training stimulus specific. Furthermore, hkBCG or hkMm training did not alter IL-1Ra levels from those of controls, although this protein is involved in the inhibition of trained immunity, and training of macrophages with uric acid downregulated its expression *in vitro*.⁴⁶

Trained immunity has traditionally been defined as the functional reprogramming of innate immune cells, leading to modifications in metabolism and an increased response toward a second challenge.⁸ In the present study, hkMm significantly increased L(+)-Lactate levels in all cases, thereby emphasizing the relation between trained immunity and metabolic reprogramming. Although lactate levels were increased in trained THP-1-derived macrophages, no differences were found in the expression of Hypoxia-inducible factor 1-alpha (HIF1 α), Hexokinase 2 (HK2), Glucose transporter 3 (GLUT3), Pyruvate kinase M2 (PKM2), Pyruvate dehydrogenase kinase 4 (PDK4), 6-phosphofructo-2-kinase/fructose-2,6-biphosphatase 3 (PFKFB3), or Phosphofructokinase (PFKP) glycolytic enzymes. The lack of differences could be due to THP-1-derived macrophages showing reduced responsiveness in terms of gene expression changes upon activation and phorbol 12-myristate 13-acetate (PMA) differentiation, when compared to that of naive primary macrophages.⁴⁷ Also, one has to bear in mind that glycolytic enzymes are also regulated post-translationally, and, therefore, certain key glycolytic enzymes could be regulated at the protein level without changes in gene expression.⁴⁸ As regards epigenetic regulation, hkMm increased H3K4me3 and H3K27ac at the promoter sites of proinflammatory genes. This observation thus highlights that trained immunity by hkMm induces epigenetic modifications. In contrast, and in line with previously published studies,²⁹ hkMm did not increase all proinflammatory cytokines after exposure to all the secondary stimuli tested. Of note, LPS is recognized by both Toll-like receptor (TLR) 4 and TLR2 in an independent manner, conferring a more robust stimulation,^{49,50} while other agents such as Mtb, *S. aureus*, SARS-CoV-2, and SIV H1N1 are detected by TLRs 2, 3, 4, 7, 8, and 9.^{51–54} These observations suggest that trained immunity may be pathogen and TLR specific.

Beyond the discovered role of hkMm on trained immunity, our results emphasize its ability to modulate proinflammatory cytokine expression. This finding is consistent with previous results, in which *M. manresensis* was shown to modulate memory-specific Tregs and IL-10 and to reduce neutrophilic infiltration and TNF- α , IFN γ , IL-6, and IL-17 production in the lungs,^{32–35} while increasing IFN γ , TNF- α , IL-6, and IL-10 levels in the spleen.³³

In our assays, inflammatory responses to inactivated virus were lower than those to LPS, *S. aureus*, or Mtb. Although we used high concentrations of inactivated viruses, the amount of TLR agonist could have been limited by the lack of viral replication. Nevertheless, given that hkMm was capable of inducing trained immunity *in vitro*, both in the THP-1 cell line and in primary monocytes in response to LPS, *S. aureus*, and Mtb, NR may have decreased the rate and severity of SARS-CoV-2 infection. This notion is in line with the proposed potential effect of BCG vaccination, given the fact that trehalose dimycolate, present in the mycobacterial cell wall, had previously demonstrated its capacity to increase the resistance against influenza virus in an experimental model.³⁷

However, the randomized, double-blind, placebo-controlled clinical trial MANRECOVID19 found that NR showed no efficacy in protecting against or reducing the severity of SARS-CoV-2 infection. Importantly, it also found no evidence of any detrimental effect of NR treatment. As a target population, we chose healthcare professionals working in the healthcare system of the Catalan Health Institute as they were expected to be highly exposed to SARS-CoV-2. However, it is necessary to take into account the progressively lower incidence of SARS-CoV-2 infection and the improvement of prophylactic measures in the health system during the study follow-up. As secondary outcomes, we also assessed the efficacy of NR at reducing the severity of SARS-CoV-2 infection, although we did not detect differences between the two groups. The lack of effect of NR described in the present study is therefore unexpected, although in line with other clinical trials assessing the effect of BCG on COVID-19.^{27–30}

Additionally, daily oral administration of a capsule of NR for 14 days did not appear to induce trained immunity *in vivo* as no enhancement of inflammatory responses was observed in peripheral blood monocytes in response to an array of secondary stimuli. Interestingly, NR increased the percentage of non-classical monocytes and CD4⁺CD25⁺ T cells. The latter are a highly active subset of memory T cells, associated with anti-inflammatory activity,^{55–59} and CD4⁺CD25⁺ CD127hi T cells might be responsible for switching a proinflammatory response to an anti-inflammatory Th2-type response.⁶⁰ As regards Treg cells, no differences were observed between groups. This finding is in contrast to our observation in previous studies, where *in vitro* purified protein derivative (PPD) stimulation of splenocytes³³ or peripheral blood monocytes³⁵ induced an increase in the PPD-specific Treg population in orally treated subjects. As regards non-classical monocytes, these cells are primarily involved in promoting the resolution of inflammation, while maintaining vascular endothelial homeostasis.⁶¹ Regarding SARS-CoV-2 infection, a study on myeloid subsets in COVID-19 patients showed a significant decrease in almost all circulating myeloid subsets, the decrease in non-classical monocytes being more pronounced in severe and critical patients, thereby indicating an association with severity.⁶² This finding is also in agreement with additional reports showing a decrease in non-classical monocyte population in severe COVID-19 patients,^{63,64} thereby reinforcing the relevance of non-classical monocyte action during SARS-CoV-2 infection. Thus, although a protective effect of NR against SARS-CoV-2 infection could not be confirmed in the clinical trial, the increase population of non-classical monocytes may confer certain protection.

Dosage and route of administration are crucial, as the beneficial effects of BCG on SARS-CoV-2 infection in mice appear when it is given intravenously and not intradermally.⁶⁵ Moreover, it is important to note that BCG vaccination was originally designed to be administered orally. Indeed, extensive experience on its protective effectiveness has been gathered in Brazil, where it has been given orally since 1925.⁶⁶ The nature of vaccines is also critical as the BCG vaccine¹⁸ and Mtb vaccine (MTBVAC)⁶⁷ are injected vaccines comprising live-attenuated virulent *Mycobacterium* strains. In contrast, NR is administered orally and *M. manresensis* is a heat-killed environmental mycobacteria. However, the capacity of intestinal bacteria-derived compounds to regulate myelopoiesis in the bone marrow, liver, and spleen is well sustained,⁶⁸ thus supporting NR's hypothetical capacity to induce trained immunity. Due to the public health emergency caused by the pandemic, we were unable to test a range of doses, and therefore we kept the safe commercial formulation and dosification.³⁴ These data are relevant as they suggest that the administration of heat-killed vs. live-attenuated bacilli affects the capacity of these bacteria to induce trained immunity *in vivo*, as previously reported for live vs. gamma-irradiated BCG.⁶⁹

In summary, here we report that hkMm induces trained immunity *in vitro* but not *in vivo* when orally administered as NR. In contrast, we observed that NR increases blood non-classical monocyte and CD4⁺CD25⁺ T cells. Taken together, our data suggest that hkMm-driven trained immunity is dosage, administration route, and pathogen specific.

Limitations of the study

We acknowledge several limitations of our work. First, we did not fully study differences in cell confluence after training and inflammatory stimuli. Nevertheless, all experiments were performed in parallel and no differences were detected by optical microscopy. Second, the *ex vivo* stimulation of monocytes from the MANRECOVID19 clinical trial was performed using frozen samples. Monocyte function after cryopreservation is controversial as some studies conclude that functional assays should be done only on fresh samples,^{70–72} while other articles report that correct cryopreservation conserves a good monocyte function.^{73–75} We chose to use frozen monocytes in order to facilitate the analysis of samples during the COVID-19 lockdown and because our prior studies confirmed frozen monocytes secreted TNF- α after LPS stimulation in a concentration-dependent manner and to a similar extent to that of freshly isolated monocytes (data not shown). Additionally, PBMCs were kept frozen until training assays. Nonetheless, flow cytometry analysis revealed that the mean viability of all samples was 95.66%, thereby adding confidence to the results reported herein.

STAR★METHODS

Detailed methods are provided in the online version of this paper and include the following:

- KEY RESOURCES TABLE
- RESOURCE AVAILABILITY
 - Lead contact
 - Materials availability
 - Data and code availability
- EXPERIMENTAL MODEL AND SUBJECT DETAILS
 - Trained immunity model in THP-1 monocytes
 - Trained immunity in primary monocytes
 - Manrecovid19 clinical trial
- METHOD DETAILS
 - Reagents
 - Monocyte isolation from buffy coats
 - Functional analyses
 - Metabolic activity assays
 - RNA extraction and quantitative RT-PCR
 - Chromatin immunoprecipitation analysis
 - Leukocyte staining for flow cytometry analysis
 - *In vitro* stimulation of monocytes from MANRECOVID19 clinical trial
 - Cytokine measurements
- QUANTIFICATION AND STATISTICAL ANALYSIS
- ADDITIONAL RESOURCES

SUPPLEMENTAL INFORMATION

Supplemental information can be found online at <https://doi.org/10.1016/j.isci.2023.106873>.

ACKNOWLEDGMENTS

We would like to thank all the volunteers for participating in this study, the investigators and study personnel, and Marco Fernández and Gerard Requena from IGTP's Flow Cytometry Platform for their support.

The MANRECOVID19 clinical trial has been sponsored by the Reig Jofre Group. This research was funded by the Consorcio Centro de Investigación Biomédica en Red (CIBERES and CIBEREHD) and the European Union's Horizon 2020 research and innovation programme under grant agreement No 847762. MDH is supported by a Margarita Salas grant from NextGenerationEU. LS-M is supported by Juan de la Cierva fellowship (FJC2019-041213-I). NI-U is supported by the Spanish Ministry of Science and Innovation (grant PID2020-117145RB-I00), EU HORIZON-HLTH-2021-CORONA-01 (grant 101046118), and institutional funding from Grifols, Pharma Mar, HIPRA, Amassence, and Palobiofarma. The Innate Immunity lab and the UTE are accredited by the Catalan Agency for Management of University and Research Grants (2017-SGR-490/

2021-SGR-01186, 2021-SGR-00931, and 2017-SGR-500/2021 SGR 00920). IGTP is a member of the CERCA network of institutes supported by the Health Department of the Government of Catalonia.

AUTHOR CONTRIBUTIONS

All the authors read and approved the final version of the manuscript. MDH, LS-M, and COV designed the study, performed research, analyzed data, and wrote and reviewed the manuscript; NR, DO, BM, AR-C, and MAP analyzed data and reviewed the manuscript; MA-S, DP-Z, JM-B, NI-U, BS, JM, SL-S, and JS contributed with participant samples and reagents and reviewed the manuscript; PT-M, ROM, and RAM designed the study and reviewed the manuscript; and P-JC, M-RS, and CV acquired financial support, designed the study, and wrote and reviewed the manuscript. MDH, LS-M, and COV contributed equally to this work.

DECLARATION OF INTERESTS

P-JC and CV are founders of Manremyc, the “Spin-off” of the Germans Trias i Pujol Research Institute (IGTP) that is developing the use of Nyaditum resae in collaboration with Reig Jofre SA. P-JC was also the CEO/CSO of Manremyc. P-JC and CV are the inventors of this food supplement.

The MANRECOVID19 clinical trial was sponsored by the Reig Jofre Group, which had no role in the study design or data collection and analysis, decision to publish, or preparation of the manuscript. All authors had full access to all the data in the study and had final responsibility for the decision to submit for publication.

Received: September 6, 2022

Revised: April 24, 2023

Accepted: May 9, 2023

Published: May 13, 2023

REFERENCES

- Gorbalenya, A.E., Baker, S.C., Baric, R.S., de Groot, R.J., Drosten, C., Gulyaeva, A.A., Haagmans, B.L., Lauber, C., Leontovich, A.M., Neuman, B.W., et al. (2020). The species Severe acute respiratory syndrome-related coronavirus: classifying 2019-nCoV and naming it SARS-CoV-2. *Nat. Microbiol.* 5, 536–544.
- World health organization weekly epidemiological update on COVID-19. Ed. 102. <https://www.who.int/publications/m/item/weekly-epidemiological-update-on-covid-19--27-july-2022>.
- Asghar, N., Mumtaz, H., Syed, A.A., Eqbal, F., Maharjan, R., Bamboria, A., and Shrehta, M. (2022). Safety, efficacy, and immunogenicity of COVID-19 vaccines; a systematic review. *Immunol. Med.* 45, 225–237.
- Madhi, S.A., Baillie, V., Cutland, C.L., Voysey, M., Koen, A.L., Fairlie, L., Padayachee, S.D., Dheda, K., Barnabas, S.L., Bhorat, Q.E., et al. (2021). Efficacy of the ChAdOx1 nCoV-19 covid-19 vaccine against the B.1.351 variant. *N. Engl. J. Med.* 384, 1885–1898.
- McCallum, M., Bassi, J., De Marco, A., Chen, A., Walls, A.C., Di Iulio, J., Tortorici, M.A., Navarro, M.J., Silacci-Fregni, C., Saliba, C., et al. (2021). SARS-CoV-2 immune evasion by the B.1.427/B.1.429 variant of concern. *Science* 373, 648–654.
- Deng, X., Garcia-Knight, M.A., Khalid, M.M., Servellita, V., Wang, C., Morris, M.K., Sotomayor-González, A., Glasner, D.R., Reyes, K.R., Gliwa, A.S., et al. (2021). Transmission, infectivity, and neutralization of a spike L452R SARS-CoV-2 variant. *Cell* 184, 3426–3437.e8.
- Zhou, D., Dejnirattisai, W., Supasa, P., Liu, C., Mentzer, A.J., Ginn, H.M., Zhao, Y., Duyvesteyn, H.M.E., Tuekprakhon, A., Nutalai, R., et al. (2021). Evidence of escape of SARS-CoV-2 variant B.1.351 from natural and vaccine-induced sera. *Cell* 184, 2348–2361.e6.
- Netea, M.G., Domínguez-Andrés, J., Barreiro, L.B., Chavakis, T., Divangahi, M., Fuchs, E., Joosten, L.A.B., van der Meer, J.W.M., Mhlanga, M.M., Mulder, W.J.M., et al. (2020). Defining trained immunity and its role in health and disease. *Nat. Rev. Immunol.* 20, 375–388.
- Kleinnijenhuis, J., Quintin, J., Preijers, F., Joosten, L.A.B., Iffrim, D.C., Saeed, S., Jacobs, C., van Loenhout, J., de Jong, D., Stunnenberg, H.G., et al. (2012). Bacille Calmette-Guérin induces NOD2-dependent nonspecific protection from reinfection via epigenetic reprogramming of monocytes. *Proc. Natl. Acad. Sci. USA* 109, 17537–17542.
- Angelidou, A., Diray-Arce, J., Conti, M.G., Smolen, K.K., van Haren, S.D., Dowling, D.J., Husson, R.N., and Levy, O. (2020). BCG as a case study for precision vaccine development: lessons from vaccine heterogeneity, trained immunity, and immune ontogeny. *Front. Microbiol.* 11, 332–416.
- Roy, A., Eisenhut, M., Harris, R.J., Rodrigues, L.C., Sridhar, S., Habermann, S., Snell, L., Mangtani, P., Adetifa, I., Lalvani, A., and Abubakar, I. (2014). Effect of BCG vaccination against Mycobacterium tuberculosis infection in children: systematic review and meta-analysis. *BMJ* 349, g4643.
- Brewer, T.F. (2000). Preventing tuberculosis with Bacillus calmette-guérin vaccine: a meta-analysis of the literature. *Clin. Infect. Dis.* 31, S64–S67.
- Setia, M.S., Steinmaus, C., Ho, C.S., and Rutherford, G.W. (2006). The role of BCG in prevention of leprosy: a meta-analysis. *Lancet Infect. Dis.* 6, 162–170.
- Zimmermann, P., Finn, A., and Curtis, N. (2018). Does BCG vaccination protect against nontuberculous mycobacterial infection? A systematic review and meta-analysis. *J. Infect. Dis.* 218, 679–687.
- Stensballe, L.G., Nante, E., Jensen, I.P., Kofoed, P.-E., Poulsen, A., Jensen, H., Newport, M., Marchant, A., and Aaby, P. (2005). Acute lower respiratory tract infections and respiratory syncytial virus in infants in Guinea-Bissau: a beneficial effect of BCG vaccination for girls. *Vaccine* 23, 1251–1257.
- de Castro, M.J., Pardo-Seco, J., and Martín-Torres, F. (2015). Nonspecific (heterologous) protection of neonatal BCG vaccination against hospitalization due to respiratory infection and sepsis. *Clin. Infect. Dis.* 60, 1611–1619.

17. Wardhana, Jim, E., Datau, E.A., Sultana, A., Mandang, V.V.V., and Jim, E. (2011). The efficacy of Bacillus Calmette-Guérin vaccinations for the prevention of acute upper respiratory tract infection in the elderly. *Acta Med. Indones.* **43**, 185–190.
18. Arts, R.J.W., Moorlag, S., Novakovic, B., Li, Y., Wang, S.Y., Oosting, M., Kumar, V., Xavier, R.J., Wijmenga, C., Joosten, L.A.B., et al. (2018). BCG vaccination protects against experimental viral infection in humans through the induction of cytokines associated with trained immunity. *Cell Host Microbe* **23**, 89–100.e5.
19. Leentjens, J., Kox, M., Stokman, R., Gerretsen, J., Diavatopoulos, D.A., van Crevel, R., Rimmelzwaan, G.F., Pickkers, P., and Netea, M.G. (2015). BCG vaccination enhances the immunogenicity of subsequent influenza vaccination in healthy volunteers: a randomized, placebo-controlled pilot study. *J. Infect. Dis.* **212**, 1930–1938.
20. Walk, J., de Bree, L.C.J., Graumans, W., Stoter, R., van Gemert, G.-J., van de Vegte-Bolmer, M., Teelen, K., Hermsen, C.C., Arts, R.J.W., Behet, M.C., et al. (2019). Outcomes of controlled human malaria infection after BCG vaccination. *Nat. Commun.* **10**, 874.
21. Giamarellos-Bourboulis, E.J., Tsilika, M., Moorlag, S., Antonakos, N., Kotsaki, A., Domínguez-Andrés, J., Kyriazopoulou, E., Gkavogianni, T., Adami, M.-E., Damoraki, G., et al. (2020). Activate: randomized clinical trial of BCG vaccination against infection in the elderly. *Cell* **183**, 315–323.e9.
22. Clinicaltrials.gov (2022). Bethesda National Library of Medicine. <https://clinicaltrials.gov/>.
23. Tsilika, M., Taks, E., Dolianitis, K., Kotsaki, A., Leventogiannis, K., Damoulari, C., Kostoula, M., Paneta, M., Adamis, G., Papanikolaou, I., et al. (2022). ACTIVATE-2: a double-blind randomized trial of BCG vaccination against COVID-19 in individuals at risk. *Front. Immunol.* **13**, 873067.
24. Pittet, L.F., Messina, N.L., Gardiner, K., Orsini, F., Abruzzo, V., Bannister, S., Bonten, M., Campbell, J.L., Croda, J., Dalcolmo, M., et al. (2021). BCG vaccination to reduce the impact of COVID-19 in healthcare workers: protocol for a randomised controlled trial (BRACE trial). *BMJ Open* **11**, e052101.
25. Madsen, A.M.R., Schaltz-Buchholzer, F., Benfield, T., Bjerregaard-Andersen, M., Dalgaard, L.S., Dam, C., Ditlev, S.B., Faizi, G., Johansen, I.S., Kofoed, P.-E., et al. (2020). Using BCG vaccine to enhance non-specific protection of health care workers during the COVID-19 pandemic: a structured summary of a study protocol for a randomised controlled trial in Denmark. *Trials* **21**, 799.
26. Junqueira-Kipnis, A.P., dos Anjos, L.R.B., Barbosa, L.C.d.S., da Costa, A.C., Borges, K.C.M., Cardoso, A.d.R.O., Ribeiro, K.M., Rosa, S.B.A., Souza, C.d.C., das Neves, R.C., et al. (2020). BCG revaccination of health workers in Brazil to improve innate immune responses against COVID-19: a structured summary of a study protocol for a randomised controlled trial. *Trials* **21**, 881.
27. ten Doesschate, T., Moorlag, S., van der Vaart, T.W., Taks, E., Debisarun, P., ten Oever, J., Bleeker-Rovers, C.P., Verhagen, P.B., Lalmohamed, A., ter Heine, R., et al. (2020). Two Randomized Controlled Trials of Bacillus Calmette-Guérin Vaccination to reduce absenteeism among health care workers and hospital admission by elderly persons during the COVID-19 pandemic: a structured summary of the study protocols for two randomised. *Trials* **21**, 481.
28. Czajka, H., Zapolnik, P., Krzych, Ł., Kmiecik, W., Stopyra, L., Nowakowska, A., Jackowska, T., Darmochwał-Kolarz, D., Szymański, H., Radziejewicz-Winnicki, I., and Mazur, A. (2022). A multi-center, randomised, double-blind, placebo-controlled phase III clinical trial evaluating the impact of BCG Re-vaccination on the incidence and severity of SARS-CoV-2 infections among symptomatic healthcare professionals during the COVID-19 pandemic. *Vaccines* **10**, 314.
29. Upton, C.M., van Wijk, R.C., Mockeliunas, L., Simonsson, U.S.H., McHarry, K., van den Hoogen, G., Müller, C., von Delft, A., van der Westhuizen, H.-M., van Crevel, R., et al. (2022). Safety and efficacy of BCG re-vaccination in relation to COVID-19 morbidity in healthcare workers: a double-blind, randomised, controlled, phase 3 trial. *eClinicalMedicine* **48**, 101414.
30. dos Anjos, L.R.B., da Costa, A.C., Cardoso, A., Guimarães, R.A., Rodrigues, R.L., Ribeiro, K.M., Borges, K.C.M., Carvalho, A., Dias, C.I.S., Rezende, A., et al. (2022). Efficacy and safety of BCG revaccination with *M. bovis* BCG moscow to prevent COVID-19 infection in health care workers: a randomized phase II clinical trial. *Front. Immunol.* **13**, 1–18.
31. Messina, N.L., Germano, S., McElroy, R., Rudraraju, R., Bonnici, R., Pittet, L.F., Neeland, M.R., Nicholson, S., Subbarao, K., Curtis, N., et al. (2022). Off-target effects of bacillus Calmette-Guérin vaccination on immune responses to SARS-CoV-2: implications for protection against severe COVID-19. *Clin. Transl. Immunol.* **11**, 1–15.
32. Rech, G., Vilaplana, C., Velasco, J., Pluvinet, R., Santín, S., Prat, C., Julián, E., Alcaide, F., Comas, I., Sumoy, L., and Cardona, P.J. (2015). Draft genome sequences of *Mycobacterium setense* strain DSM-45070 and the nonpathogenic strain manresensis, isolated from the bank of the cardener river in manresa, Catalonia, Spain. *Genome Announc.* **3**, e01485-14.
33. Cardona, P., Marzo-Escartín, E., Tapia, G., Díaz, J., García, V., Varela, I., Vilaplana, C., and Cardona, P.J. (2015). Oral administration of heat-killed *Mycobacterium manresensis* delays progression toward active tuberculosis in C3HeB/FeJ mice. *Front. Microbiol.* **6**, 1482–1513.
34. Turck, D., Castenmiller, J., De Henuaw, S., Hirsch-Ernst, K.I., Kearney, J., Maciuk, A., Mangelsdorf, I., McArdle, H.J., Naska, A., Pelaez, C., et al. (2019). Safety of heat-killed *Mycobacterium setense manresensis* as a novel food pursuant to Regulation (EU) 2015/2283. *EFSA J.* **17**. <https://doi.org/10.2903/j.efs.2019.5824>.
35. Montané, E., Barriocanal, A.M., Arellano, A.L., Valderrama, A., Sanz, Y., Perez-Alvarez, N., Cardona, P., Vilaplana, C., and Cardona, P.-J. (2017). Pilot, double-blind, randomized, placebo-controlled clinical trial of the supplement food Nyaditum resae® in adults with or without latent TB infection: safety and immunogenicity. *PLoS One* **12**, e0171294.
36. Dulberger, C.L., Rubin, E.J., and Boutte, C.C. (2020). The mycobacterial cell envelope — a moving target. *Nat. Rev. Microbiol.* **18**, 47–59.
37. Masahi, K.N., Brehmer, W., Lange, W., Werner, H., and Ribi, E. (1985). Trehalose dimycolate from various mycobacterial species induces differing anti-infectious activities in combination with muramyl dipeptide. *Infect. Immun.* **50**, 938–940.
38. Bekkering, S., Blok, B.A., Joosten, L.A.B., Riksen, N.P., Van Crevel, R., and Netea, M.G. (2016). In vitro experimental model of trained innate immunity in human primary monocytes. *Clin. Vaccine Immunol.* **23**, 926–933.
39. Bekkering, S., Domínguez-Andrés, J., Joosten, L.A.B., Riksen, N.P., and Netea, M.G. (2021). Trained immunity: reprogramming innate immunity in health and disease. *Annu. Rev. Immunol.* **39**, 667–693.
40. Zingaropoli, M.A., Nijhawan, P., Carraro, A., Pasculli, P., Zuccalà, P., Perri, V., Marocco, R., Kertusha, B., Siccardi, G., Del Borgo, C., et al. (2021). Increased sCD163 and sCD14 plasmatic levels and depletion of peripheral blood pro-inflammatory monocytes, myeloid and plasmacytoid dendritic cells in patients with severe COVID-19 pneumonia. *Front. Immunol.* **12**, 1–12.
41. Jeljeli, M., Riccio, L.G.C., Doridot, L., Chêne, C., Nicco, C., Chouzenoux, S., Deletang, Q., Allanore, Y., Kavian, N., and Batteux, F. (2019). Trained immunity modulates inflammation-induced fibrosis. *Nat. Commun.* **10**, 5670.
42. Yao, Y., Jeyanathan, M., Haddadi, S., Barra, N.G., Vaseghi-Shanjani, M., Damjanovic, D., Lai, R., Afkhami, S., Chen, Y., Dvorkin-Gheva, A., et al. (2018). Induction of autonomous memory alveolar macrophages requires T cell help and is critical to trained immunity. *Cell* **175**, 1634–1650.e17.
43. Murphy, D.M., Cox, D.J., Connolly, S.A., Breen, E.P., Brugman, A.A., Phelan, J.J., Keane, J., and Basdeo, S.A. (2023). Trained immunity is induced in humans after immunization with an adenoviral vector COVID-19 vaccine. *J. Clin. Invest.* **133**, e162581.
44. Garcia-Valtanan, P., Guzman-Genuino, R.M., Williams, D.L., Hayball, J.D., and Diener, K.R. (2017). Evaluation of trained immunity by β -1, 3 (d)-glucan on murine monocytes *in vitro*

- and duration of response *in vivo*. *Immunol. Cell Biol.* 95, 601–610.
45. Leonhardt, J., Große, S., Marx, C., Siwczak, F., Stengel, S., Bruns, T., Bauer, R., Kiehnopf, M., Williams, D.L., Wang, Z.-Q., et al. (2018). *Candida albicans* β -glucan differentiates human monocytes into a specific subset of macrophages. *Front. Immunol.* 9, 1–13.
 46. Crişan, T.O., Cleophas, M.C.P., Oosting, M., Lemmers, H., Toenhake-Dijkstra, H., Netea, M.G., Jansen, T.L., and Joosten, L.A.B. (2016). Soluble uric acid primes TLR-induced proinflammatory cytokine production by human primary cells via inhibition of IL-1Ra. *Ann. Rheum. Dis.* 75, 755–762.
 47. Maeß, M.B., Wittig, B., Cignarella, A., and Lorkowski, S. (2014). Reduced PMA enhances the responsiveness of transfected THP-1 macrophages to polarizing stimuli. *J. Immunol. Methods* 402, 76–81.
 48. Tong, X., Zhao, F., Mancuso, A., Gruber, J.J., and Thompson, C.B. (2009). The glucose-responsive transcription factor ChREBP contributes to glucose-dependent anabolic synthesis and cell proliferation. *Proc. Natl. Acad. Sci. USA* 106, 21660–21665.
 49. Francisco, S., Billod, J.-M., Merino, J., Punzón, C., Gallego, A., Arranz, A., Martín-Santamaria, S., and Fresno, M. (2021). Induction of TLR4/TLR2 interaction and heterodimer formation by low endotoxic atypical LPS. *Front. Immunol.* 12, 748303–748312.
 50. Hirschfeld, M., Ma, Y., Weis, J.H., Vogel, S.N., and Weis, J.J. (2000). Cutting edge: repurification of lipopolysaccharide eliminates signaling through both human and murine toll-like receptor 2. *J. Immunol.* 165, 618–622.
 51. Zhang, J., Miao, J., Hou, J., and Lu, C. (2015). The effects of H3N2 swine influenza virus infection on TLRs and RLRs signaling pathways in porcine alveolar macrophages. *Virol. J.* 12, 61.
 52. Faridgohar, M., and Nikouejad, H. (2017). New findings of Toll-like receptors involved in *Mycobacterium tuberculosis* infection. *Pathog. Glob. Health* 111, 256–264.
 53. Askarian, F., Wagner, T., Johannessen, M., and Nizet, V. (2018). *Staphylococcus aureus* modulation of innate immune responses through Toll-like (TLR), (NOD)-like (NLR) and C-type lectin (CLR) receptors. *FEMS Microbiol. Rev.* 42, 656–671.
 54. Manik, M., and Singh, R.K. (2022). Role of toll-like receptors in modulation of cytokine storm signaling in SARS-CoV-2-induced COVID-19. *J. Med. Virol.* 94, 869–877.
 55. Baecher-Allan, C., Brown, J.A., Freeman, G.J., and Hafler, D.A. (2001). CD4+ CD25 high regulatory cells in human peripheral blood. *J. Immunol.* 167, 1245–1253.
 56. Cao, D., Malmström, V., Baecher-Allan, C., Hafler, D., Klareskog, L., and Trollmo, C. (2003). Isolation and functional characterization of regulatory CD25brightCD4+ T cells from the target organ of patients with rheumatoid arthritis. *Eur. J. Immunol.* 33, 215–223.
 57. Lundgren, A., Suri-Payer, E., Enarsson, K., Svennerholm, A.-M., and Lundin, B.S. (2003). *Helicobacter pylori*-specific CD4+ CD25 high regulatory T cells suppress memory T-cell responses to *H. pylori* in infected individuals. *Infect. Immun.* 71, 1755–1762.
 58. Liyanage, U.K., Moore, T.T., Joo, H.-G., Tanaka, Y., Herrmann, V., Doherty, G., Drebin, J.A., Strasberg, S.M., Eberlein, T.J., Goedegebuure, P.S., and Linehan, D.C. (2002). Prevalence of regulatory T cells is increased in peripheral blood and tumor microenvironment of patients with pancreas or breast adenocarcinoma. *J. Immunol.* 169, 2756–2761.
 59. Woo, E.Y., Yeh, H., Chu, C.S., Schlienger, K., Carroll, R.G., Riley, J.L., Kaiser, L.R., and June, C.H. (2002). Cutting edge: regulatory T cells from lung cancer patients directly inhibit autologous T cell proliferation. *J. Immunol.* 168, 4272–4276.
 60. Narsale, A., Moya, R., and Davies, J.D. (2018). Human CD4+ CD25+ CD127hi cells and the Th1/Th2 phenotype. *Clin. Immunol.* 188, 103–112.
 61. Narasimhan, P.B., Marcovecchio, P., Hamers, A.A.J., and Hedrick, C.C. (2019). Nonclassical monocytes in health and disease. *Annu. Rev. Immunol.* 37, 439–456.
 62. Sánchez-Cerrillo, I., Landete, P., Aldave, B., Sánchez-Alonso, S., Sánchez-Azofra, A., Marcos-Jiménez, A., Avalos, E., Alcaraz-Serna, A., de los Santos, I., Mateu-Albero, T., et al. (2020). COVID-19 severity associates with pulmonary redistribution of CD11c+ DCs and inflammatory transitional and nonclassical monocytes. *J. Clin. Invest.* 130, 6290–6300.
 63. Gatti, A., Radrizani, D., Viganò, P., Mazzone, A., and Brando, B. (2020). Decrease of non-classical and intermediate monocyte subsets in severe acute SARS-CoV-2 infection. *Cytometry A* 97, 887–890.
 64. Mueller, K.A.L., Langnau, C., Günter, M., Pöschel, S., Gekeler, S., Petersen-Uribe, Á., Kreisselmeier, K.-P., Klingel, K., Bösmüller, H., Li, B., et al. (2021). Numbers and phenotype of non-classical CD14dimCD16+ monocytes are predictors of adverse clinical outcome in patients with coronary artery disease and severe SARS-CoV-2 infection. *Cardiovasc. Res.* 117, 224–239.
 65. Hilligan, K.L., Namasivayam, S., Clancy, C.S., O'Mard, D., Oland, S.D., Robertson, S.J., Baker, P.J., Castro, E., Garza, N.L., Lafont, B.A.P., et al. (2022). Intravenous administration of BCG protects mice against lethal SARS-CoV-2 challenge. *J. Exp. Med.* 219. <https://doi.org/10.1084/jem.20211862>.
 66. Benévolo-de-Andrade, T.C., Monteiro-Maia, R., Cosgrove, C., and Castello-Branco, L.R.R. (2005). BCG Moreau Rio de Janeiro: an oral vaccine against tuberculosis - review. *Mem. Inst. Oswaldo Cruz* 100, 459–465.
 67. Tarancón, R., Domínguez-Andrés, J., Uranga, S., Ferreira, A.V., Groh, L.A., Domenech, M., González-Camacho, F., Riksen, N.P., Aguilo, N., Yuste, J., et al. (2020). New live attenuated tuberculosis vaccine MTBVAC induces trained immunity and confers protection against experimental lethal pneumonia. *PLoS Pathog.* 16, e1008404.
 68. Gorjifard, S., and Goldszmid, R.S. (2016). Microbiota—myeloid cell crosstalk beyond the gut. *J. Leukoc. Biol.* 100, 865–879.
 69. Arts, R.J.W., Blok, B.A., Aaby, P., Joosten, L.A.B., de Jong, D., van der Meer, J.W.M., Benn, C.S., van Crevel, R., and Netea, M.G. (2015). Long-term *in vitro* and *in vivo* effects of γ -irradiated BCG on innate and adaptive immunity. *J. Leukoc. Biol.* 98, 995–1001.
 70. Weinberg, A., Betensky, R.A., Zhang, L., and Ray, G. (1998). Effect of shipment, storage, anticoagulant, and cell separation on lymphocyte proliferation assays for human immunodeficiency virus-infected patients. *Clin. Diagn. Lab. Immunol.* 5, 804–807.
 71. Betensky, R.A., Connick, E., Devers, J., Landay, A.L., Nokta, M., Plaeger, S., Rosenblatt, H., Schmitz, J.L., Valentine, F., Wara, D., et al. (2000). Shipment impairs lymphocyte proliferative responses to microbial antigens. *Clin. Diagn. Lab. Immunol.* 7, 759–763.
 72. Costantini, A., Mancini, S., Giuliodoro, S., Butini, L., Regnery, C.M., Silvestri, G., and Montroni, M. (2003). Effects of cryopreservation on lymphocyte immunophenotype and function. *J. Immunol. Methods* 278, 145–155.
 73. Reimann, K.A., Chernoff, M., Wilkening, C.L., Nickerson, C.E., and Landay, A.L. (2000). Preservation of lymphocyte immunophenotype and proliferative responses in cryopreserved peripheral blood mononuclear cells from human immunodeficiency virus type 1-infected donors: implications for multicenter clinical trials. *Clin. Diagn. Lab. Immunol.* 7, 352–359.
 74. Zhao, Y., Glesne, D., and Huberman, E. (2003). A human peripheral blood monocyte-derived subset acts as pluripotent stem cells. *Proc. Natl. Acad. Sci. USA* 100, 2426–2431.
 75. Ruitenberg, J.J., Mulder, C.B., Maino, V.C., Landay, A.L., and Ghanekar, S.A. (2006). VACUTAINER CPT and Ficoll density gradient separation perform equivalently in maintaining the quality and function of PBMC from HIV seropositive blood samples. *BMC Immunol.* 7, 11.
 76. Pan, W., Hao, S., Zheng, M., Lin, D., Jiang, P., Zhao, J., Shi, H., Yang, X., Li, X., and Yu, Y. (2020). Oat-derived β -glucans induced trained immunity through metabolic reprogramming. *Inflammation* 43, 1323–1336.
 77. Harris, P.A., Taylor, R., Thielke, R., Payne, J., Gonzalez, N., and Conde, J.G. (2009). Research electronic data capture (REDCap)—a metadata-driven methodology and workflow process for providing translational

- research informatics support. *J. Biomed. Inform.* 42, 377–381.
78. Harris, P.A., Taylor, R., Minor, B.L., Elliott, V., Fernandez, M., O'Neal, L., McLeod, L., Delacqua, G., Delacqua, F., Kirby, J., and Duda, S.N.; REDCap Consortium (2019). The REDCap consortium: building an international community of software platform partners. *J. Biomed. Inform.* 95, 103208.
79. Rodon, J., Muñoz-Basagoiti, J., Perez-Zsolt, D., Noguera-Julian, M., Paredes, R., Mateu, L., Quiñones, C., Perez, C., Erkizia, I., Blanco, I., et al. (2021). Identification of plitidepsin as potent inhibitor of SARS-CoV-2-induced cytopathic effect after a drug repurposing screen. *Front. Pharmacol.* 12, 1–12.
80. Darnell, M.E.R., Subbarao, K., Feinstone, S.M., and Taylor, D.R. (2004). Inactivation of the coronavirus that induces severe acute respiratory syndrome, SARS-CoV. *J. Virol. Methods* 121, 85–91.
81. López-Serrano, S., Cordoba, L., Pérez-Maillo, M., Pleguezuelos, P., Remarque, E.J., Ebsen, T., Guzmán, C.A., Christensen, D., Segalés, J., and Darji, A. (2021). Immune responses to pandemic H1N1 influenza virus infection in pigs vaccinated with a conserved hemagglutinin HA1 peptide adjuvanted with CAF@01 or CDA/ α GalCerMPEG. *Vaccines* 9, 751.
82. Reed, L.J., and Muench, H. (1938). A simple method of estimating fifty per cent endpoints. *Am. J. Epidemiol.* 27, 493–497.
83. Martín, B., Pappa, S., Díez-Villanueva, A., Mallona, I., Custodio, J., Barrero, M.J., Peinado, M.A., and Jordà, M. (2020). Tissue and cancer-specific expression of D1EXF is epigenetically mediated by an Alu repeat. *Epigenetics* 15, 765–779.

STAR★METHODS

KEY RESOURCES TABLE

REAGENT or RESOURCE	SOURCE	IDENTIFIER
Antibodies		
FITC Mouse Anti-Human CD14	BD Biosciences	Cat# 555397, RRID:AB_395798
CD14 Spark Blue 550	BioLegend	Cat# 367148, RRID:AB_2832724
CD3 PerCP	BD Biosciences	Cat# 345766, RRID:AB_2783791
CD25 PE	BD Biosciences	Cat# 557138, RRID:AB_396584
CD19 PE-Cy7	BD Biosciences	Cat# 560911, RRID:AB_10562390
CD56 AF647	BD Biosciences	Cat# 563443, RRID:AB_2738209
CD127 APC-R700	BD Biosciences	Cat# 565185, RRID:AB_2739099
HLA-DR APC-F750	BioLegend	Cat# 307658, RRID:AB_2572101
CD11c BUV661	BD Biosciences	Cat# 612967, RRID:AB_2870241
CD39 BV421	BioLegend	Cat# 328213, RRID:AB_10933084
CD8 BV510	BD Biosciences	Cat# 563919, RRID:AB_2722546
CD4 BV650	BD Biosciences	Cat# 563875, RRID:AB_2744425
CD163 BV711	BD Biosciences	Cat# 563889, RRID:AB_2738469
CD16 BV786	BD Biosciences	Cat# 563689, RRID:AB_2744299
CD11b BB515	BD Biosciences	Cat# 564517, RRID:AB_2744271
Anti-Histone H3 (tri methyl K4) antibody - ChIP Grade	Abcam	Cat# ab8580, RRID:AB_306649
Anti-Histone H3 (acetyl K27) antibody - ChIP Grade	Abcam	Cat# ab4729, RRID:AB_2118291
Normal Rabbit Serum	Jackson Immunoresearch	Cat# 011-000-120, RRID:AB_2337123
Bacterial and virus strains		
<i>Mycobacterium manresensis</i>	Experimental Tuberculosis Unit, IGTP	Strain CECT 8638
<i>Staphylococcus aureus</i>	Microbiology Laboratory, Germans Trias i Pujol University Hospital	Strain H-9477
<i>Mycobacterium tuberculosis</i>	Microbiology Laboratory, Germans Trias i Pujol University Hospital	Strain H37Rv Pasteur
SARS-CoV-2	Pathogen Immunity, Signaling and Therapeutic Applications, IrsiCaixa AIDS Research Institute	GISAID ID EPI_ISL_510689
Swine influenza virus	IRTA-UAB Research Unit in Animal Health. Animal Health Research Center	Strain A/Swine/Spain/SF11131/2007H1N1
Biological samples		
BCG vaccine	BCG-Medac, Medac	PA Number: PA 0623/004/001
Nyaditum resae®	Reig Jofre	N/A
Buffy coats	Banc de Sang i Teixits, Barcelona	N/A
Peripheral blood samples from healthcare workers	Germans Trias i Pujol University Hospital	NCT04452773
Chemicals, peptides, and recombinant proteins		
LPS (from <i>Escherichia coli</i> O55:B5)	Sigma-Aldrich	L2880
Perfect-Count™ Microspheres	Cytognos	CYT-PCM-50-R
RosetteSep Human CD3 Depletion Cocktail	StemCell Technologies	15661
DMEM with 4.5 g/L glucose, L-glutamine, sodium pyruvate	Corning	10-013-CM
RPMI 1640 with L-Glutamine	Corning	10-040-CV
Fetal Bovine Serum EU-approved	Tico Europe	FBSEU500
Penicillin-Streptomycin	Sigma-Aldrich	P0781

(Continued on next page)

Continued

REAGENT or RESOURCE	SOURCE	IDENTIFIER
PMA	Sigma-Aldrich	P8139
Endotoxin-Free Dulbecco's PBS	Sigma-Aldrich	TMS-012
Ficoll® Paque Plus	Cytiva	17-1440-02
Percoll	Cytiva	17-0891-02
Human Serum	Sigma-Aldrich	H4522
GlutaMAX	Thermo Scientific	35050038
Sodium Pyruvate	Thermo Scientific	11360039
True-Stain Monocyte Blocker™	BioLegend	426101
Critical commercial assays		
Lactate Assay Kit	Sigma-Aldrich	MAK064
Human TNF α ELISA Set	BD OptEIA™	555212
Human IL-6 ELISA Set	BD OptEIA™	555220
Human IL-1 β ELISA Set II	BD OptEIA™	557953
Human IL-10 ELISA Set	BD OptEIA™	555157
Human IL-1ra ELISA Kit	Abcam	ab211650
TMB	Sigma-Aldrich	T0440
LowCell# CHIP kit protein A	Diagenode	C01010070
NuceloSpin Gel and PCR Clean-up (50)	Cultek	22740609.50
QIAzol Lysis Reagent	Qiagen	79306
miRNeasy Mini Kit	Qiagen	217004
EcoDry™ Premix	Takara	639549
Deposited data		
SARS-CoV-2	http://gisaid.org	ID: EPI_ISL_510689
Experimental models: Cell lines		
Human: THP-1	ATCC	TIB-202; RRID: CVCL_0006
Oligonucleotides		
Primers, see Table S1	Invitrogen	N/A
Software and algorithms		
REDCap (Research Electronic Data Capture)	REDCap consortium	RRID: SCR_003445
ImageJ	Open source Java	RRID: SCR_003070
FlowJo™ v10.8	BD Biosciences	RRID: SCR_008520
GraphPad Prism, version 9.0	GraphPad Software	RRID: SCR_002798
R statistical package, v4.1	The R Project for Statistical Computing	RRID: SCR_001905
Other		
Flat-bottom 96-well plate	Thermo Scientific	732-2721
BD Scientific Canto II Flow Cytometer	BD Biosciences	RRID: SCR_018056
BD LSRFortessa Fortessa Flow Cytometer	BD Biosciences	RRID: SCR_019601
Cytek Aurora Spectral Analyzer	Cytek Biosciences	RRID: SCR_019826
LightCycler® 480 PCR system	Roche	05015278001

RESOURCE AVAILABILITY

Lead contact

Further information and requests for resources and reagents should be directed to and will be fulfilled by the lead contact, Maria-Rosa Sarrias (mrsarrias@igtp.cat).

Materials availability

All reagents and materials used in this manuscript are available upon request or prepared to be available from commercial sources.

Data and code availability

Data reported in this paper will be shared by the [lead contact](#) upon request. This study did not generate any unique datasets or code. Any additional information required to reanalyse the data reported in this work paper is available from the [lead contact](#) upon request.

EXPERIMENTAL MODEL AND SUBJECT DETAILS

Using the THP-1 cell line and primary samples from buffy coats, we examined the capacity of heat-killed *M. mannesensis* (hkMm) to induce trained immunity *in vitro*. To this end, we analyzed modifications of proinflammatory cytokines, metabolic activity, and epigenetic marks. We also conducted the MANRECOVID19 clinical trial and tested the capacity of hkMm to train immunity *in vivo* and its ability to modify circulating peripheral blood populations. To this end, we used samples from healthy volunteers and characterized whole blood leukocyte pattern and the production of proinflammatory cytokines in response to a set of inflammatory stimuli.

Trained immunity model in THP-1 monocytes

Before training, THP-1 cells (ATCC TIB-202; RRID: CVCL_0006) were cultured in DMEM medium containing 4.5 g/L glucose, 584 mg/L L-glutamine and 110 mg/L sodium pyruvate (Corning, NY, USA) supplemented with 10% heat-inactivated fetal bovine serum (FBS) (Lonza, Switzerland), 1% penicillin-streptomycin (Sigma-Aldrich, Spain), at 37°C and 5% CO₂ for at least one week. The THP-1 cell line was tested and found to be mycoplasma-free. The trained immunity model using this cell line was performed as described previously.⁷⁶ Briefly, THP-1 cells were first seeded into a flat-bottom 96-well plate (Corning, NY, USA) at a density of 50,000 cells/well, either with 200 µL of culture medium alone as negative control, heat-killed BCG (hkBCG, BCG-Medac, Medac, Germany; 10⁶ cfu/mL) as positive control, or heat-killed *M. mannesensis* (strain CECT 8638; 10⁶ cfu/mL) for 24 h. During this training period, cell proliferation did not differ between groups as shown by cell confluence analysis by optical microscopy. Cells were then washed twice with warm PBS (by centrifugation at 400g for 5 min and extracting the supernatant) and differentiated into macrophages in the presence of 10% FBS DMEM supplemented with 10 ng/mL phorbol 12-myristate 13-acetate (PMA) for 32 h. After washing twice with warm PBS (by centrifugation at 400g for 5 min and extracting the supernatant), macrophages were left to rest for 24 h. They were then restimulated for 24 h with either heat-killed *Staphylococcus* (*S.*) *aureus* (hkS. aureus 5x10⁶ cfu/mL), Lipopolysaccharides (LPS) (10 ng/mL), heat-killed *Mycobacterium* (*M.*) *tuberculosis* (hkMtb 10⁶ cfu/mL), inactivated SARS-CoV-2 (InSARS-CoV-2 0.218 ng nucleocapsid/mL), inactivated swine influenza virus (InSIV) H1N1 (10^{4.29} TCID₅₀/mL), or with medium alone as negative control. Before the addition of inflammatory stimuli, brightfield images were acquired using Leica DM IL LED microscope with an ×20 objective. A total of six independent experiments, each in triplicate, were performed. Cellular supernatants were aliquoted and stored at −20°C until further analysis. To quantify differences in cell size, the area of untrained, and hkBCG- and hkMm-trained THP-1 cells was measured using ImageJ software (RRID:SCR_003070).

Trained immunity in primary monocytes

Monocytes purified as described below (see Monocyte isolation from buffy coats in [method details](#)) were incubated for 24 h with 200 µL of culture medium alone as negative control, hkBCG (10⁶ cfu/mL) as positive control, or hkMm (10⁶ cfu/mL) in complete RPMI (supplemented with 1% penicillin-streptomycin, 10% heat-inactivated human male AB serum (both from Sigma-Aldrich, Spain), 1 mM sodium pyruvate and 2 mM GlutaMax (both from Life Technologies, Germany)). Cells were washed with warm PBS and left to rest for 5 days in complete RPMI, with a change of media on day 3. After the resting period, macrophages were restimulated for 24 h either with hkS. aureus (5x10⁶ cfu/mL), LPS (10 ng/mL), hkMtb (10⁶ cfu/mL), InSARS-CoV-2 (0.218 ng nucleocapsid/mL), InSIV H1N1 (10^{4.29} TCID₅₀/mL), or with RPMI alone as negative control. Experiments were performed in triplicate. Cellular supernatants were aliquoted and stored at −20°C until further analysis.

Manrecovid19 clinical trial

Design and participants

Healthcare workers, expected to be highly exposed to COVID-19, at five public healthcare centers in Catalonia, namely CAP El Maresme, CAP Sant Felix, CAP Santa Coloma de Gramanet, CAP Cornellà, and

Germans Trias i Pujol University Hospital, were enrolled in this randomized, double-blind, placebo-controlled trial between 14 July 2020 and 4 April 2021. A total of 320 individuals were assessed for eligibility to participate in the study; 317 were randomized to receive NR (n = 214) or placebo (n = 103), and they composed the ITT sample. The PP sample was composed by 198 participants; 131 in the NR group and 67 in the placebo group. A flowchart of study participants is shown in [Figure 4](#). All participants received information about the study procedures and signed the consent form. They optionally signed another consent form for storage and future use of unused biological samples collected during the trial. Those participants who also volunteered for the trained immunity sub-study signed the corresponding consent form. The Experimental Tuberculosis Unit (UTE) coordinated the trial, while the laboratory of Innate Immunity at Germans Trias Research Institute (IGTP) served as a central laboratory for the study. This study is registered with ClinicalTrials.gov (NCT04452773).

Inclusion and exclusion criteria were

Inclusion criteria

1. Sign the Informed Consent before initiating the selection procedures.
2. Health system workers in contact with subjects potentially infected with SARS-CoV-2.
3. Age \geq 18 years.
4. Availability to meet the requirements of the protocol.
5. Negative Rapid Serological Test of SARS-CoV-2.

Exclusion criteria

1. Previous SARS-CoV-2 infection.
2. Pregnancy or breastfeeding.
3. Suspected of having active viral or bacterial infection.
4. Symptoms compatible with COVID-19, despite a negative PCR test.
5. Vaccination in the last 4 weeks or planned vaccination during the study period, regardless of the type of vaccine.
6. Participation in research that requires experimental intervention (does not include observational studies) in the previous month before signing the Consent or during the study.
7. Severely immunocompromized people. This exclusion category includes:
 - a. Subjects with human immunodeficiency virus (HIV-1).
 - b. Neutropenic subjects with less than 500 neutrophils/mm³.
 - c. Subjects with solid organ transplantation.
 - d. Subjects with bone marrow transplantation.
 - e. Subjects undergoing chemotherapy.
 - f. Subjects with primary immunodeficiency.
 - g. Severe lymphopenia with less than 400 lymphocytes/mm³.
 - h. Treatment with any anti-cytokine therapy.
 - i. Oral treatment with steroids, defined as daily doses of 10 mg prednisone or equivalent for more than 3 months.
8. Malignancy, or active solid or non-solid lymphoma in the previous two years.
9. BCG vaccination in the last 10 years.
10. Treatment with Manremyc for the last 6 months.
11. Chloroquine or hydroxychloroquine administration in the last two weeks.

12. Direct involvement in the design or execution of the MANRECOVID19 clinical trial.
13. Retirement, transfer, long-term leave (>1 month) due to scheduled surgery or any other event that makes it impossible to work in person at your health center during the months following the recruitment to the study.
14. Employee at the health center <22 h per week.
15. Do not have a smartphone.
16. Detection by the investigator of lack of knowledge or willingness to participate and comply with all requirements of the protocol.
17. Any other findings that, at the discretion of the investigator, may compromise compliance with the protocol or that may influence significantly the interpretation or the results of the effects of probiotic.

Data collection

The clinical trial data collection had a nine-month duration. Study data were collected and managed using REDCap electronic data capture tools hosted at Fundació Institut Universitari per a la recerca an l'Atenció Primària de Salut Jordi Gol i Gurina (IDIAPJGol).^{77,78} REDCap (Research Electronic Data Capture) is a secure, web-based software platform designed to support data capture for research studies, providing 1) an intuitive interface for validated data capture; 2) audit trails for tracking data manipulation and export procedures; 3) automated export procedures for seamless data downloads to common statistical packages; and 4) procedures for data integration and interoperability with external sources.

Randomization and masking

A specific case report form (CRF) was designed for randomization and data collection. Participants were randomly assigned to one of the study arms, Nyaditum resae or placebo, in a 2:1 proportion. The blinding was ensured through a list of codes of the treatment assigned to each participant by order of inclusion. The code was registered in the CRF during the baseline visit. The treatments, which were administered orally once a day for two weeks (14 days), comprised a capsule of Nyaditum resae, consisting of $10^{3.5}$ heat-killed bacilli of *M. manresensis*, or placebo, which were the excipients also present in NR, basically mannitol.

Outcomes and follow-up

The primary efficacy variable was the cumulative incidence of documented SARS-CoV-2 infection; assessed by a positive serology at the end of the study or a positive RT-PCR test during the study period. The secondary variables of efficacy assessed in the study were: sick leave due to documented SARS-CoV-2 infection, number of days of sick leave due to the quarantine for acute respiratory symptoms, fever or documented SARS-CoV-2 infection, quarantine due to a close contact with a subject with SARS-CoV-2 infection out of the center, professional category (general practitioner, nurse, management and services' staff, etc.), number of days of self-reported fever ($\geq 38^\circ\text{C}$), cumulative incidence of self-reported acute respiratory symptoms, number of days of self-reported acute respiratory symptoms, pneumonia incidence (X-rays confirmed), cumulative incidence of death caused by documented SARS-CoV-2 infection, cumulative incidence of ICU admission due to documented SARS-CoV-2 infection, number of days of ICU admission due to documented SARS-CoV-2 infection, cumulative incidence of mechanical ventilation due to documented SARS-CoV-2 infection, number of days of mechanical ventilation due to documented SARS-CoV-2 infection, cumulative incidence of hospital admission due to documented SARS-CoV-2 infection, number of days of hospital admission due to documented SARS-CoV-2 infection, incidence of SARS-CoV-2 antibodies at the end of the study period, type of antibodies detected (IgG and IgM), and level of SARS-CoV-2 antibodies at the end of the study period.

Face-to-face visits were limited to obtention of the consent, laboratory tests and treatment dispensing. Study procedures and variables collected in each visit are listed in Table S3. The baseline visit was a face-to-face visit for inclusion in the study (day 1), when the treatment was assigned according to the randomization after meeting the inclusion criteria and none of the exclusion criteria. A rapid antigenic test (RAT) and a serological blood test were conducted, along with ruling out COVID-19 symptoms. The second visit was a phone call at day 15 (± 3 days), where symptoms and treatment tolerance and compliance were evaluated. The third visit was conducted at day 60 (± 3 days) and consisted of a phone call to

assess symptoms. The final visit at day 120 (± 3 days) was a face-to-face meeting where a new serological blood test was done. Participants were also contacted through WhatsApp or other messaging server to remind them about their participation in the study and to evaluate the symptoms and the adverse events that had occurred since the last visit (days 30, 45, 75, 90, 105 ± 3 days). If participants presented symptoms compatible with a SARS-CoV-2 infection at any moment during the study period, they could contact the investigator directly. Further phone calls were performed on a weekly basis to assess severity and duration of the symptoms, and participants were invited to complete a phone questionnaire until the symptoms had disappeared, and/or they had returned to work.

Also, in the participants of the sub-study, 20 mL of peripheral blood was collected by venipuncture in Vacutainer Heparine tubes at both visits (day 0 and day 15 after intervention). Of these, 1 mL was used for immediate whole blood surface staining for flow cytometry analysis. The remaining volume (19 mL) was used to isolate PBMCs by Ficoll density gradient centrifugation. Cells were frozen and stored in liquid nitrogen at a density of 5×10^6 until further analysis.

All studies involving human samples were conducted following the Declaration of Helsinki principles, current legislation on the confidentiality of personal data, and ICH Good Clinical Practice Guidelines, and were approved by the Human Ethics Committee of the Germans Trias i Pujol. The MANRECOVID19 clinical trial protocol and its subsequent amendments were evaluated and approved by the Independent Ethics Committee (IEC) of the Germans Trias i Pujol University Hospital (PI-20-165) and by the IEC of IDIAPJGol (20/090-AC).

METHOD DETAILS

Reagents

M. manresensis (strain CECT 8638) was grown and subcultured in 7H11 plates and processed as previously described.³³ Colony-forming units (cfu) were counted, heat-killed through incubation for 30 min at 80°C, aliquoted, and stored at -20°C .

The BCG vaccine (BCG-Medac, Medac, Germany) was diluted with endotoxin-free PBS, heat-killed through incubation for 20 min at 80°C, and stored at -20°C .

Staphylococcus (S.) aureus (strain H-9477 from the Microbiology Laboratory at the Germans Trias i Pujol University Hospital) was grown on Luria-Bertani (LB) broth until it reached the log phase. Bacteria were counted, heat-killed through incubation for 30 min at 80°C, and stored at -20°C .

Lipopolysaccharides (LPS) from *Escherichia coli* O55:B5 (Sigma-Aldrich, Germany) were resuspended in endotoxin-free H₂O and stored at -20°C .

Mycobacterium tuberculosis H37Rv Pasteur strain (Mtb) was grown in 250 mL PYREX bottles in a shaking incubator at 37°C and 120 rpm in Middlebrook 7H9 broth (Becton Dickinson, Spain) supplemented with 0.2% glycerol, 0.5% albumin-dextrose catalase (Becton Dickinson, Spain) and 0.05% Tween 80. Bottle caps were left half open to allow unlimited O₂ availability. Mycobacteria were grown to mid-log phase, counted, heat-killed through incubation for 30 min at 80°C, and stored at -20°C .

SARS-CoV-2 was isolated from a nasopharyngeal swab collected from a COVID-19 patient in March 2020 in Spain, which was processed as previously described.⁷⁹ Viral stock was inactivated for 20 min at 65°C and titrated on Vero E6 cells (ATCC Cat# CRL-1586, RRID:CVCL_0574) to confirm viral inactivation as compared to an untreated viral stock, as previously described.⁸⁰ The genomic sequence was deposited in the GISAID repository (<http://gisaid.org>) under accession ID EPI_ISL_510689. The amount of nucleoprotein was measured with a SARS-CoV-2 nucleocapsid protein high-sensitivity quantitative ELISA (ImmunoDiagnostics, Hong Kong), following the manufacturer's protocol. Aliquots were stored at -80°C . The Biological Biosafety Committee of the Germans Trias i Pujol Research Institute approved the execution of SARS-CoV-2 experiments at the BSL3 laboratory of the Center for Bioimaging and Comparative Medicine.

A/Swine/Spain/SF11131/2007H1N1 swine influenza virus (SIV) strain was obtained using Madin-Darby Canine Kidney (MDCK) cells (ATCC Cat# CCL-34, RRID:CVCL_0422), as described before.⁸¹ To this end, cells were inoculated with a viral MOI of 0.001 with 10 $\mu\text{g}/\text{mL}$ porcine trypsin (Sigma-Aldrich, Spain) to

obtain the desired concentration after two days. Subsequently, cultures were frozen to allow the rupture of infected cells and were then centrifuged. Titration of the inoculum was performed by serial dilutions in MDCK cells and calculated using the Reed and Muench method.⁸² The final titer of the prepared SIV inoculum was $10^{8.29}$ TCID₅₀/mL. Supernatants containing the virus were then inactivated by incubation for 1 h at 60°C in a water bath and then stored at –80°C.

Monocyte isolation from buffy coats

Buffy coats from healthy blood donors (Banc de Sang i Teixits, Barcelona, Spain) were diluted in PBS and incubated with RosetteSep Human CD3 Depletion Cocktail (StemCell Technologies, Vancouver, Canada) to remove T cells. Monocyte-enriched suspensions were then acquired as previously described.³⁸ Briefly, peripheral blood mononuclear cells (PBMCs) were isolated by Ficoll-Paque Plus (GE Healthcare, UK) density gradient centrifugation, washed with PBS, and counted by flow cytometry using Perfect-Count microspheres (Cytognos, Spain). PBMCs were then layered on top of a hyperosmotic Percoll solution (Sigma-Aldrich, Spain), and monocytes were isolated from the interphase by density gradient centrifugation, washed with cold PBS, stained with FITC Mouse Anti-Human CD14 (BD Biosciences Cat# 555397, RRID:AB_395798), and counted by flow cytometry using Perfect-Count microspheres (Cytognos, Spain). Monocytes were resuspended in RPMI culture medium (Corning, NY, USA) supplemented with 1% penicillin-streptomycin and 10% heat-inactivated human male AB serum (both from Sigma-Aldrich, Spain), seeded into a flat-bottom 96-well plate (Corning, NY, USA) at a density of 100,000 cells/well, and incubated at 37°C 5% CO₂ for 1 h 30 min. Non-adherent cells were washed out with warm PBS. After Ficoll and Percoll purification, 59.37% of the cells were CD14⁺. After adherence, CD14⁺ cells increased to a 78.71% of the total.

Functional analyses

After the induction of trained immunity in both THP-1 cells and primary monocytes from buffy coats, we determined modifications of proinflammatory cytokine secretion by ELISA, metabolic activity by L(+)-Lactate measurements, as well as TNF α , IL-6, and IL-1 β promoters epigenetic marks (H3K4me3 and H3K27ac) by chromatin immunoprecipitation.

Metabolic activity assays

As metabolic marker, L(+)-Lactate from supernatants was analyzed using a colorimetric assay (Sigma-Aldrich, Germany), following the manufacturer's recommendations. In brief, 50 μ L of reaction mix (containing 2 μ L of lactate enzyme and 2 μ L of lactate probe) was added to 50 μ L of each sample diluted 1:20. Absorbance was measured every 5 min for 30 min at 570 nm using a SPECTROstar Nano Microplate Reader (BMG LABTECH, Germany). Background values were subtracted from all readings, and all experiments were performed in triplicate. Final values were expressed as μ M of lactate.

RNA extraction and quantitative RT-PCR

After training, THP-1-derived macrophages were disrupted with QIAzol Lysis Reagent (Qiagen), and RNA was extracted using the miRNeasy Mini Kit (Qiagen). Total RNA (500 ng) was reverse transcribed using the RNA to cDNA EcoDry Premix (Clontech). Each RT reaction was then amplified in a LightCycler 480 PCR system (Roche) using the KAPA SYBR Fast Master Mix (KAPA Biosystems). Samples were incubated for an initial denaturation at 95°C for 5 min, then 40 PCR cycles were performed using the following conditions: 95°C for 10 s, 60°C for 20 s, and 72°C for 10 s. The primer pairs used in the study are listed in [Table S1](#). Gene expression values were normalized to the expression levels of HUP1 and to the mean of untrained THP-1 cells.

Chromatin immunoprecipitation analysis

After training, primary monocytes from buffy coats were collected to perform chromatin immunoprecipitation (ChIP). Next, 100,000 monocytes from three samples were crosslinked with 1% formaldehyde and lysed, as previously described.³³ Fixed cell preparations were sonicated with a Bioruptor Pico device (Diagenode, Belgium) using 10 cycles of 30 s on and 30 s off. Sonicated lysates were immunoprecipitated using LowCell# ChIP kit protein A (Diagenode, Belgium), following the manufacturer's protocol. We used ChIP-grade antibodies (1–5 μ g) specific for H3K4me3 (Abcam Cat# ab8580, RRID:AB_306649) and H3K27ac (Abcam Cat# ab4729, RRID:AB_2118291) as active marks, and normal rabbit serum IgG (011-000-120, Jackson ImmunoResearch) as negative control. Equal amounts of immunoprecipitated DNA were used for qPCR and

they were normalized to total chromatin input (6% of the total chromatin). Glyceraldehyde-3-phosphate dehydrogenase (GAPDH) was used as a qPCR positive control of active marks. The primer pairs used are listed in [Table S1](#).

Leukocyte staining for flow cytometry analysis

Before staining, 1 mL of peripheral whole blood was processed with red blood cell lysing solution BD Pharm Lyse (BD Biosciences, CA, USA), following the manufacturer's instructions. Cells were resuspended in PBS-2% heat-inactivated FBS (Lonza, Switzerland) and counted using Perfect Count microspheres (Cytognos, Spain). Viability staining was then performed using Live/Dead Fixable Blue (ThermoFisher, L23105). A total of 2×10^6 cells were resuspended in PBS-2%FBS, containing 10% True-Stain Monocyte Blocker (BioLegend, 426101), and incubated for 20 min at room temperature with the following antibodies: CD14 Spark Blue 550 (BioLegend Cat# 367148, RRID:AB_2832724); CD3 PerCP (BD Biosciences Cat# 345766, RRID:AB_2783791); CD25 PE (BD Biosciences Cat# 557138, RRID:AB_396584); CD19 PE-Cy7 (BD Biosciences Cat# 560911, RRID:AB_10562390); CD56 AF647 (BD Biosciences Cat# 563443, RRID:AB_2738209); CD127 APC-R700 (BD Biosciences Cat# 565185, RRID:AB_2739099); HLA-DR APC-F750 (BioLegend Cat# 307658, RRID:AB_2572101); CD11c BUV661 (BD Biosciences Cat# 612967, RRID:AB_2870241); CD39 BV421 (BioLegend Cat# 328213, RRID:AB_10933084); CD8 BV510 (BD Biosciences Cat# 563919, RRID:AB_2722546); CD4 BV650 (BD Biosciences Cat# 563875, RRID:AB_2744425); CD163 BV711 (BD Biosciences Cat# 563889, RRID:AB_2738469); CD16 BV786 (BD Biosciences Cat# 563689, RRID:AB_2744299); and CD11b BB515 (BD Biosciences Cat# 564517, RRID:AB_2744271). Cells were then washed twice with PBS at 420 g for 5 min and fixed in PBS-1% PFA buffer for 10 min at room temperature. Cells were acquired using a 5-laser Full Spectrum Aurora Flow Cytometry System (RRID: SCR_019826), with a minimum of 3×10^5 events acquired for each sample. Controls included unstained and single stained samples for unmixing raw data. Results were analyzed using SpectroFlo (Cytek Biosciences, CA, USA) and FlowJo (RRID: SCR_008520) software.

In vitro stimulation of monocytes from MANRECOVID19 clinical trial

Frozen PBMCs from each donor at 0 and 15 days were thawed simultaneously. Recovered monocytes were washed, and counted as described above. PBMCs containing 50,000 monocytes were resuspended in RPMI culture medium supplemented with 100 U/ml penicillin and streptomycin, 10% FBS (Lonza, Switzerland), and 5% human AB serum, 100 U/mL penicillin, and seeded into 96-wells plates. Cell culture was then enriched in monocytes by allowing cells to adhere to polystyrene flat-bottom plates for 30 min in a 5% CO₂ incubator at 37°C. Non-adherent cells were washed out with warm PBS and adherent cells were incubated in complete RPMI for 24 h. After the resting period, macrophages were stimulated either with 100 ng/mL LPS, 10^6 cfu/mL hkMtb, 10^7 cfu/mL *hkS. aureus*, 2.25 pfu/mL InSARS-CoV-2, 6.85×10^3 pfu/ml InSIVs or with RPMI only as negative control for 24 h. Cellular supernatants were aliquoted and stored at -20°C until further analysis.

Cytokine measurements

Cytokine levels were assessed by ELISA, following the manufacturer's instructions, using OptEIA TNF α , IL-6, IL-1 β , and IL-10 kits (BD Biosciences, CA, USA). Values below the detection limit of the test were replaced by the detection limit of the test, namely 1.56 pg/mL, 0.47 pg/mL, 1.95 pg/mL, and 2.93 pg/mL, respectively. IL-1ra was analyzed also by using a simple step ELISA kit (Abcam, the Netherlands), with 0.976 pg/mL as limit of detection. All samples were analyzed in triplicate. For the MANRECOVID19 biological samples, a fold change in concentration (day 15/day 0) was calculated.

QUANTIFICATION AND STATISTICAL ANALYSIS

In vitro assays were analyzed using the Kolmogorov-Smirnov test to assess normal distribution, and given that the data were not following a Gaussian distribution, a Wilcoxon matched-pairs signed-rank test comparing the raw values to those of the untreated controls. A two-tailed p value below 0.05 was considered statistically significant.

Clinical trial analyses were conducted with the statistical software R (v4.1, RRID:SCR_001905), with a significance level of 5%. The main numerical variables are described by means of dispersion measures and the categorical variables through frequencies. Comparison of means (t-test or similar) or comparison of distributions (chi-square or similar) were used for bivariate comparisons between groups. All participants who met inclusion criteria were analyzed as Intention to treat (ITT) population. The per protocol (PP) population

was composed by those participants with a confirmed negative result in the SARS-CoV-2 test before the study initiation, who completed the final study visit without significant deviations from the protocol and had not received any COVID-19 vaccine before the study end.

The main variable was considered dichotomous (0: no infection, 1: infection) and, consequently, logistic regression models were fitted using as independent variables those presenting a significant difference in the previously bivariate comparisons. In addition, we also added demographics, clinical variables and/or those considered relevant in the adjustment of the odds ratio (OR) estimators. The Goodness-of-fit (GoF) of the final model was analyzed using the residuals. The results of the analyses were tabulated with descriptive data for the main outcome, univariable ORs and adjusted ORs with the 95% confidence interval (CI) and their p value. Time-to-event variables of interest (e.g., days to complete disappearance of symptoms) were analyzed using between-group survival models based on Log rank test from the estimated Kaplan-Meier curves and Cox proportional hazards models. Kaplan-Meier were also used to estimate the median life and its 95% CI. Time to event between groups were compared using Cox proportional hazards models adjusted for the different baseline variables of interest. The hazard ratio (HR) point estimator, and its 95% CI, was tabulated together with the total number of events observed throughout the study. A validation of the Cox models was carried out using residuals analysis. Specifically, the following assumptions were validated: proportional Risks by Schoenfeld residuals, and effect of outlier observations by Residual deviance.

Inflammatory response and circulating immune cell populations were collected at baseline and 15 days post-treatment administration, and the analyses were conducted for the fold-change (FC) between samples at day 15 against their baseline. Inflammatory response and circulating immune cell populations of healthy volunteers were described as median and interquartile range (IQR) and frequencies with its percentages. The median FCs between treatment arms was compared by means of the Mann-Whitney test under a significance level of 0.05. Analyses were conducted using the R statistical package (v4.1, RRID:SCR_001905) and GraphPad Prism (version 9.0, RRID:SCR_002798).

ADDITIONAL RESOURCES

Clinical Trial was registered with the code NCT04452773 at ClinicalTrials.gov.